STATISTICS, OPTIMIZATION AND INFORMATION COMPUTING
Stat., Optim. Inf. Comput., Vol. **13**, June 2025, pp 2353–2381.
Published online in International Academic Press (www.IAPress.org)

A Novel Fréchet-Poisson Model: Properties, Applications under Extreme Reliability Data, Different Estimation Methods and Case Study on Strength-Stress Reliability Analysis

Mohamed Ibrahim[1,*], S. I. Ansari[2], Abdullah H. Al-Nefaie[1], Ahmad M. AboAlkhair[1], Mohamed S. Hamed[3] and Haitham M Yousof[4]

[1]*Department of Quantitative Methods, School of Business, King Faisal University, Al Ahsa 31982, Saudi Arabia*
[2]*Department of Business Administration, Azad institute of Engineering and Technology, Lucknow, India*
[3]*Department of Business Administration, Gulf Colleges, KSA*
[4]*Department of Statistics, Mathematics and Insurance, Faculty of Commerce, Benha University, Egypt*

Abstract A new compound extension of the Fréchet distribution is introduced and studied. Some of its properties including moments, incomplete moments, probability weighted moments, moment generating function, stress strength reliability model, residual life and reversed residual life functions are derived. The mean squared errors (MSEs) for some estimation methods including maximum likelihood estimation (MLE), Cramér–von Mises (CVM) estimation, Bootstrapping (Boot.) estimation and Kolmogorov estimates (KE) method are used to estimate the unknown parameter via a simulation study. Two real applications are presented for comparing the estimation methods. Another two real applications are presented for comparing the competitive models. The nonparametric Hill estimator under the breaking stress of carbon fibers is estimated using the tail index (TIx) of the new model. Finally, a case study on reliability analysis of composite materials for aerospace applications is presented.

Keywords Fréchet Distribution; Nonparametric Hill estimator; Zero Truncated Poisson Distribution; Maximum Likelihood; Tail Index.

AMS 2010 subject classifications 62N01; 62N02; 62E10.

DOI: 10.19139/soic-2310-5070-2463

1. Introduction and physical motivation

Consider a sequence of independent and identically distributed random variables (iid RV) $X_1, X_2, ..., X_m$, all sharing the same cumulative distribution function (CDF). One of the most interesting statistics is the sample maximum

$$\varsigma_m \left(X_i | i = 1, 2, ...m\right) = \max\left\{X_1, X_2, ..., X_m\right\}.$$

One is keen on the behaviour of ς_m as the sample size m increases to infinity, then

$$\begin{aligned} \Pr\left(\varsigma_m \leq x\right) &= \Pr\left(X_1 \leq x, X_2 \leq x, ..., X_m \leq x\right) \\ &= \Pr\left(X_1 \leq x\right) \Pr\left(X_2 \leq x\right) ... \Pr\left(X_m \leq x\right) \\ &= F\left(x\right) F\left(x\right) ... F\left(x\right) = F^m\left(x\right). \end{aligned}$$

*Correspondence to: Mohamed Ibrahim (Email: miahmed@kfu.edu.sa). Department of Quantitative Methods, School of Business, King Faisal University, Al Ahsa 31982, Saudi Arabia.

ISSN 2310-5070 (online) ISSN 2311-004X (print)

Assume there are sequences of constants $(\tau_m > 0)$ and (ℓ_m) such that

$$\Pr\left[\frac{1}{\tau_m}(\varsigma_m - \ell_m) \leq x\right] \to G(x) \text{ as } m \to \infty,$$

then if $G(x)$ is a non-degenerate distribution function, then it will belong to one of the three following fundamental types of classic extreme value families which are Type **I** (Gumbel distribution), Type **II** (Fréchet (Fr) distribution) and Type **III** (Weibull distribution). The extreme value theory concentrates on the behavior of the block maxima or minima. The EVT was presented first by Fréchet [41] and Fisher and Tippett [39], then continued by Von Mises [93] and then completed by Gnedenko [42], Von Mises [94], among others. In past ten years, researchers have extended and generalized the classical extreme value models to accommodate more real data structures and improve their flexibility. For example: Korkmaz et al. [57], Yousof et al. [103], Al-Babtain et al. [24], Elsayed and Yousof [37], Elgohari and Yousof [35] and Verster and Mbongo [92].

A r.v. X is said to have the Fréchet (Fr) distribution if its probability density function (PDF) and CDF are given by

$$g(x) = ba^b x^{-(b+1)} \varrho(x|a,b), \tag{1}$$

and

$$G(x) = \varrho(x|a,b), \tag{2}$$

respectively, where $a > 0, b > 0, x > 0$, $\varrho(x|a,b) = \exp\left[-\left(ax^{-1}\right)^b\right]$, a is a scale parameter and b is a shape parameter. For $a = 1$, we have the one parameter Fr distribution. For $b = 2$, we have the Inverse Rayleigh (IR) distribution. For $b = 1$, we have the inverse Exponential (IE) distribution. Recent advancements in extending the Fréchet distribution have significantly enhanced its flexibility and applicability, as demonstrated by several key studies. Ahmed and Yousof [23] introduced a group acceptance sampling plan based on percentiles for the Weibull Fréchet (WFr) model, offering a robust framework for quality control in industrial settings by effectively controlling producer's and consumer's risks. Ibrahim et al. [54] proposed a three-parameter xgamma Fréchet distribution, which combines the xgamma family with the Fréchet model to capture diverse shapes and tail behaviors, while exploring various estimation techniques such as maximum likelihood, least squares, and Bayesian methods, and validating its superior fit through real applications. Salah et al.[80] developed an expanded Fréchet model that incorporates additional parameters and copula functions to account for dependence structures in multivariate data, investigating its mathematical properties and demonstrating its effectiveness through simulation studies and practical applications in fields like environmental science and finance. Yousof et al. [107] focused on a two-parameter xgamma Fréchet distribution, providing characterizations, reliability measures, and copula-based extensions, while comparing classical estimation methods using simulated datasets and showcasing its applicability in reliability analysis. Lastly, Jahanshahi et al. [55] introduced the Burr X Fréchet model, which integrates the Burr X and Fréchet distributions to handle heavy-tailed and asymmetric data, exploring both classical inference and Bayesian estimation methods and highlighting its utility in environmental sciences and engineering. Collectively, these studies contribute to the growing body of literature on Fréchet-based models by introducing innovative extensions, examining comprehensive estimation techniques, and validating their practical applications across diverse disciplines, thereby enriching the theoretical foundations of extreme value theory and expanding its real relevance. In fact, the statistical literature contains many works closely related to the distributions of the theory of extended values, and all of these works are considered useful either in terms of applications or in terms of statistical theory. Among these works, see [91], [53], [15], [46], [13], [14] and [69].

Recentely, Aryal and Yousof [25] introduced and studied a new flexible compound family of distributions called exponentiated generalized G Poisson (EGGP) family. The CDF and PDF of the EGGP family given by

$$F(x) = \mathbf{c}_{[\lambda]}^{-1}\left[1 - \exp\left(-\lambda\left\{1 - [1 - G(x)]^{\alpha}\right\}^{\beta}\right)\right], \tag{3}$$

where $\alpha > 0, \beta > 0, \lambda \in \mathbf{R} - \{\mathbf{0}\}, \mathbf{x} \in \mathbf{R}$, $\mathbf{c}_{[\lambda]} = [1 - \exp(-\lambda)]$ and

$$f(x) = \alpha\beta\lambda \mathbf{c}_{[\lambda]}^{-1} \frac{g(x)\left[1 - G(x)\right]^{\alpha-1}\left\{1 - \left[1 - G(x)\right]^{\alpha}\right\}^{\beta-1}}{\exp\left(\lambda\left\{1 - \left[1 - G(x)\right]^{\alpha}\right\}^{\beta}\right)}, \tag{4}$$

respectively. For $\beta = 1$ we have the exponentiated G Poisson (EGP) class of distributions and for $\alpha = 1$ we have the generalized G Poisson (GGP) class of distributions both of which are embedded in EGGP class. Using (1) and (3), we derive a new compound Fr distribution called exponentiated generalized Fréchet Poisson (EGFrP) model with CDF that can be expressed as

$$F_{\underline{\Psi}}(x) = \frac{1 - \exp\left[-\lambda\left(1 - \left\{1 - \varrho(x|a,b)\right\}^{\alpha}\right)^{\beta}\right]}{\mathbf{c}_{[\lambda]}}, \tag{5}$$

where $\underline{\Psi} = (\alpha, \beta, \lambda, a, b)$, $\alpha > 0$, $\beta > 0$, $\lambda \in \mathbf{R} - \{\mathbf{0}\}$, $a > 0, b > 0, x > 0$ and the corresponding PDF can be written as

$$f_{\underline{\Psi}}(x) = \alpha\beta\lambda b a^{b} \frac{x^{-(b+1)}\varrho(x|a,b)}{\mathbf{c}_{[\lambda]}\left\{1 - \varrho(x|a,b)\right\}^{1-\alpha}} \frac{\left(1 - \left\{1 - \varrho(x|a,b)\right\}^{\alpha}\right)^{\beta-1}}{\exp\left[\lambda\left(1 - \left\{1 - \varrho(x|a,b)\right\}^{\alpha}\right)^{\beta}\right]}. \tag{6}$$

Table 1: Sub-models of the EGFrP model.

α	β	λ	a	b	Reduced model	CDF
				2	EGIRP	$\frac{1-\exp\left[-\lambda(1-\{1-\varrho(x\|a,2)\}^{\alpha})^{\beta}\right]}{\mathbf{c}_{[\lambda]}}$
				1	EGIEP	$\frac{1-\exp\left(-\lambda\{1-[1-\varrho(x\|a,1)]^{\alpha}\}^{\beta}\right)}{\mathbf{c}_{[\lambda]}}$
			1		EGFrP	$\frac{1-\exp\left[-\lambda(1-\{1-\varrho(x\|1,b)\}^{\alpha})^{\beta}\right]}{\mathbf{c}_{[\lambda]}}$
	1				EFrP	$\frac{1-\exp[-\lambda(1-\{1-\varrho(x\|a,b)\}^{\alpha})]}{\mathbf{c}_{[\lambda]}}$
	1			2	EIRP	$\frac{1-\exp[-\lambda(1-\{1-\varrho(x\|a,2)\}^{\alpha})]}{\mathbf{c}_{[\lambda]}}$
	1			1	EIEP	$\frac{1-\exp[-\lambda(1-\{1-\varrho(x\|a,1)\}^{\alpha})]}{\mathbf{c}_{[\lambda]}}$
	1		1		EFrP	$\frac{1-\exp[-\lambda(1-\{1-\varrho(x\|1,b)\}^{\alpha})]}{\mathbf{c}_{[\lambda]}}$
1					GFrP	$\frac{1-\exp\left[-\lambda(1-\{1-\varrho(x\|a,b)\})^{\beta}\right]}{\mathbf{c}_{[\lambda]}}$
1				2	GIRP	$\frac{1-\exp\left[-\lambda(1-\{1-\varrho(x\|a,2)\})^{\beta}\right]}{\mathbf{c}_{[\lambda]}}$
1				1	GIEP	$\frac{1-\exp\left[-\lambda(1-\{1-\varrho(x\|a,1)\})^{\beta}\right]}{\mathbf{c}_{[\lambda]}}$
1			1		GFrP	$\frac{1-\exp\left[-\lambda(1-\{1-\varrho(x\|1,b)\})^{\beta}\right]}{\mathbf{c}_{[\lambda]}}$
1	1				FrP	$\frac{1-\exp[-\lambda\{\varrho(x\|a,b)\}]}{\mathbf{c}_{[\lambda]}}$
1	1			2	IRP	$\frac{1-\exp[-\lambda\{\varrho(x\|a,2)\}]}{\mathbf{c}_{[\lambda]}}$
1	1			1	IEP	$\frac{1-\exp(-\lambda\{\varrho(x\|a,1)\})}{\mathbf{c}_{[\lambda]}}$

Some important extensions of the Fréchet distribution can be cited, see for example Yousof et el. [95], Yousof et al. [96] and Yousof et al. ([99], [104], [108] and [107]) among others.

2. TIx

The TIx is a measure of how heavy the tails of the distribution are, and it is typically derived by examining the asymptotic decay rate of the survival function $\overline{F_{\underline{\Psi}}(x)}|x \to \infty = 1 - F_{\underline{\Psi}}(x)$, where $F_{\underline{\Psi}}(x)$ is CDF. For large values

of x, note that $x^{-1} \to 0$. Therefore, we can expand the quantity $\varrho\left(x|a,b\right)$ using a Taylor approximation, where

$$\overline{\varrho\left(x|a,b\right)}|x \to \infty \approx \left(ax^{-1}\right)^{b},$$

the the TIx for the new can then expressed as

$$\text{TIx} = \alpha b\left(2-\beta\right)+1, \tag{7}$$

where b conrols the power-law decay rate of the tail, α influences the exponentiation of the tail behavior and β modifies the overall shape of the distribution, including its tail weight. The TIx plays a crucial role in VaR analysis, particularly when using the EGFrP model. The Value at Risk (VaR) indicator a widely used risk measure in economy, finance, reliability and insurance to quantify the potential loss in value of a risky asset or portfolio over a specific time horizon at a given confidence level. The TIx determines the heaviness of the tails of the distribution, which directly impacts the estimation of extreme losses and thus the accuracy of VaR calculations. In financial and actuarial contexts, heavy-tailed distributions are critical because they better capture the occurrence of rare but catastrophic events (e.g., market crashes, natural disasters). Accurate modeling of these extreme events is essential for reliable VaR estimation. At high confidence levels (CLs) (like, γ=0.95 or γ=0.99), the contribution of the tail region becomes dominant in VaR calculations. For heavy-tailed distributions (TIx is too much small), the VaR increases significantly at higher CLs because the probability of extreme losses does not diminish rapidly. For light-tailed distributions (TIx is very large), the VaR grows more slowly as the confidence level increases, reflecting the reduced likelihood of extreme events. This sensitivity of VaR to the tail index highlights the importance of accurately estimating TIx in the EGFrP model. On the other hand, the VaR at a confidence level γ (e.g., γ=0.95 or γ=0.99) is defined as

$$\text{VaR}=F_{\underline{\boldsymbol{\Psi}}}^{-1}\left(1-\gamma\right) \tag{8}$$

where $F_{\underline{\boldsymbol{\Psi}}}^{-1}\left(\alpha^{*}\right)$ is the quantile function of the distribution corresponding to probability α^{*}. For heavy-tailed distributions like the EGFrP, the quantile function can often be approximated using the tail behavior of the distribution. For heavy-tailed distributions, we have

$$\overline{F_{\underline{\boldsymbol{\Psi}}}\left(x\right)}|x \to \infty = C \times x^{\text{TIx}}, \tag{9}$$

where $C > 0$ is a normalization constant, then

$$\overline{F_{\underline{\boldsymbol{\Psi}}}\left(\alpha^{*}\right)}|x \to \infty = \left(\frac{1}{1-\alpha^{*}}C\right)^{\frac{1}{\alpha b(2-\beta)+1}}, \tag{10}$$

Using the above relationship, the VaR at confidence level γ can be approximated as

$$\text{VaR}=\left(\frac{1}{\gamma}C\right)^{\frac{1}{\alpha b(2-\beta)+1}}.$$

For large x, the exponential term $\exp\left[-\lambda\left(1-\left\{1-\varrho\left(x|a,b\right)\right\}^{\alpha}\right)^{\beta}\right]$ approaches 1, so the dominant term in $\overline{F_{\underline{\boldsymbol{\Psi}}}\left(\alpha^{*}\right)}$ is proportional to $x^{-\alpha b(2-\beta)+1}$. Thus, Using the inverse of (5), we get

$$\text{VaR}=\left(\alpha\beta\lambda b a^{\alpha b}\frac{1}{\left[\alpha b\left(2-\beta\right)\right]\left(1-\gamma\right)\mathbf{c}_{[\lambda]}}\right)^{\frac{1}{\alpha b(2-\beta)+1}}.$$

3. Nonparametric Hill estimator

The Hill estimator is a widely used method for estimating the TIx of heavy-tailed distributions. It is particularly suited for datasets where the tail behavior dominates, and it provides an empirical estimate of the tail index based

on the largest observations in the dataset. The nonparametric Hill estimator can be expressed as

$$\widehat{\text{TIx}}_{\text{Hill}} = \overline{Z}^{-1}, \tag{11}$$

where

$$\overline{Z} = \frac{1}{n}\sum_{i=0}^{n} \log\left[\frac{X_{(i)}}{X_{(n)}}\right]. \tag{12}$$

where n is the number of top-order statistics used in the estimation., $X_{(i)}$ refers to the ith largest observation. and $X_{(n)}$ refers to the The nth largest observation. For more finalcial and related VaR applications see [10], [85], [87], [86], [89], [106], [109], [90].

4. Mathematical Properties

4.1. Useful expansions

Using the power series expansion of $\exp(x)$ the PDF in (6) can be expressed as

$$\begin{aligned} f(x) &= \alpha\beta b a^b \mathbf{c}_{[\lambda]}^{-1} x^{-(b+1)} \varrho(x|a,b)\{1-\varrho(x|a,b)\}^{\alpha-1} \\ &\quad \times \sum_{\kappa_1=0}^{\infty} \frac{(-1)^{\kappa_1}}{\kappa_1!\lambda^{-\kappa_1-1}} \left(1-\{1-\varrho(x|a,b)\}^{\alpha}\right)^{\beta(\kappa_1+1)-1}. \end{aligned}$$

Using the series expansion

$$\left(1-\frac{1}{\xi_2}\xi_1\right)^{\xi_3}|_{\frac{\xi_1}{\xi_2}<1,\xi_3>0} = \sum_{d=0}^{\infty} \frac{(-1)^d \,\mathbf{\Gamma}(1+\xi_3)}{d!\,\mathbf{\Gamma}(1+\xi_3-d)} \left(\frac{1}{\xi_2}\xi_1\right)^d,$$

the previous equation can be expressed as

$$f(x) = \sum_{\kappa_3=0}^{\infty} \zeta_{\kappa_3} \pi_{\kappa_3^*}(x;a,b)|_{\kappa_3^*=\kappa_3+1}, \tag{13}$$

where

$$\zeta_{\kappa_3} = \frac{\alpha\beta(-1)^{\kappa_3}}{\mathbf{c}_{[\lambda]}\kappa_3^*} \sum_{\kappa_1,\kappa_2=0}^{\infty} \frac{(-1)^{\kappa_1+\kappa_2}}{\kappa_1!\lambda^{-\kappa_1-1}} \binom{\beta(\kappa_1+1)-1}{\kappa_2} \binom{\alpha(\kappa_2+1)-1}{\kappa_3},$$

and

$$\pi_{\kappa_3^*}(x;a,b) = \kappa_3^* b a^b x^{-(b+1)} \exp\left[-\kappa_3^*\left(ax^{-1}\right)^b\right]$$

is the Fr density with scale parameter $a\kappa_3^{*\frac{1}{b}}$ and shape parameter b. By integrating (13), we obtain the mixture representation of $F(x)$ as

$$F(x) = \sum_{\kappa_3=0}^{\infty} \zeta_{\kappa_3} \Pi_{\kappa_3^*}(x;a,b),$$

where

$$\Pi_{\kappa_3^*}(x;a,b) = \exp\left[-\kappa_3^*\left(ax^{-1}\right)^b\right]$$

is the CDF of the Fr model with scale parameter $a\kappa_3^{*\frac{1}{b}}$ and shape parameter b. Equation (13) reveals that the EGFrP density function is a linear combination of Fr densities. Thus, some structural properties of the new family such as the ordinary and incomplete moments and generating function can be immediately obtained from well-established properties of the Fr distribution.

4.2. General properties

The r^{th} ordinary moment of X is given by

$$\mu'_{r,X} = \mathbf{E}(X^r) = \int_{-\infty}^{\infty} x^r \, f(x) \, dx.$$

Using (13), we obtain

$$\mu'_{r,X} = \sum_{\kappa_3=0}^{\infty} \zeta_{\kappa_3} a^r \kappa_3^{*\frac{r}{b}} \mathbf{\Gamma}\left(1 - \frac{r}{b}\right) |_{b>r}, \tag{14}$$

where $\mathbf{\Gamma}(\tau) = \int_0^{\infty} x^{\tau-1} \exp(-t)\, dx$. Setting $r = 1$ in (14), we have the mean of X as

$$\mathbf{E}(X) = \mu'_{1,X} = \sum_{\kappa_3=0}^{\infty} \zeta_{\kappa_3} a \kappa_3^{*\frac{1}{b}} \mathbf{\Gamma}\left(1 - \frac{1}{b}\right) |_{b>1}.$$

The skewness and kurtosis can be calculated from the ordinary moments using well-known relationships. We can obtain skewness and kurtosis measures using the quantile new model. The Bowley's skewness measure is given by

$$\text{Skewness} = \frac{\mathbf{Q}\left(\frac{3}{4}\right) - 2\mathbf{Q}\left(\frac{1}{2}\right) + \mathbf{Q}\left(\frac{1}{4}\right)}{-\mathbf{Q}\left(\frac{1}{4}\right) + \mathbf{Q}\left(\frac{3}{4}\right)},$$

and the Moors's kurtosis measure is

$$\text{Kurtosis} = \frac{\mathbf{Q}\left(\frac{7}{8}\right) + \mathbf{Q}\left(\frac{3}{8}\right) - \mathbf{Q}\left(\frac{1}{8}\right) - \mathbf{Q}\left(\frac{5}{8}\right)}{-\mathbf{Q}\left(\frac{2}{8}\right) + \mathbf{Q}\left(\frac{6}{8}\right)}.$$

These two measures enjoys the advantage of having less sensitivity to outliers. Moreover, they do exist for the certain model without moments. Both measures equal zero for the normal distribution. 3-dimentional (3D) plots of skewness and kurtosis of the new model are presented in Figure 6 and Figure 2. This plot indicates that both measures depends on the shape parameters a and b.

4.3. Moment generating function (MGF)

We can find the MGF, *say* $M_X(t) = \mathbf{E}[\exp(tX)]$, using a different method, the first method is given by

$$M_X(t) = \sum_{r=0}^{\infty} \frac{t^r}{r!} \mu_r^{'} = \sum_{\kappa_3, r=0}^{\infty} \frac{t^r}{r!} \zeta_{\kappa_3} a^r \kappa_3^{*\frac{r}{b}} \mathbf{\Gamma}\left(1 - \frac{r}{b}\right) |_{b>r}.$$

The second method, consider the Wright generalized hypergeometric function defined by

$${}_{[p]}\Psi_{[\mathbf{q}]}\left[\begin{array}{c} a_1, A_1, \ldots, a_p, A_p \\ b_1, B_1, \ldots, b_{\mathbf{q}}, B_{\mathbf{q}} \end{array} ; x\right] = \sum_{n=0}^{\infty} \frac{\prod_{\xi=1}^{p} \mathbf{\Gamma}(a_\xi + A_\xi\, n)}{\prod_{\xi=1}^{\mathbf{q}} \mathbf{\Gamma}(b_\xi + B_\xi\, n)} \frac{x^n}{n!}.$$

Then, we can write the MGF of (1) as

$$M_X(t) = {}_{[1]}\Psi_{[0]}\left[\begin{array}{c} \left(1, -\frac{1}{b}\right) \\ \_ \end{array} ; a\, t\right]. \tag{15}$$

Combining (7) and (9), we obtain the MGF of X, say $M_X(t)$, as

$$M_X(t) = \sum_{\kappa_3=0}^{\infty} \zeta_{\kappa_3} \; {}_{[1]}\Psi_{[0]}\left[\begin{array}{c} \left(1, -\frac{1}{b}\right) \\ \_ \end{array} ; a \kappa_3^{*\frac{1}{b}}\, t\right].$$

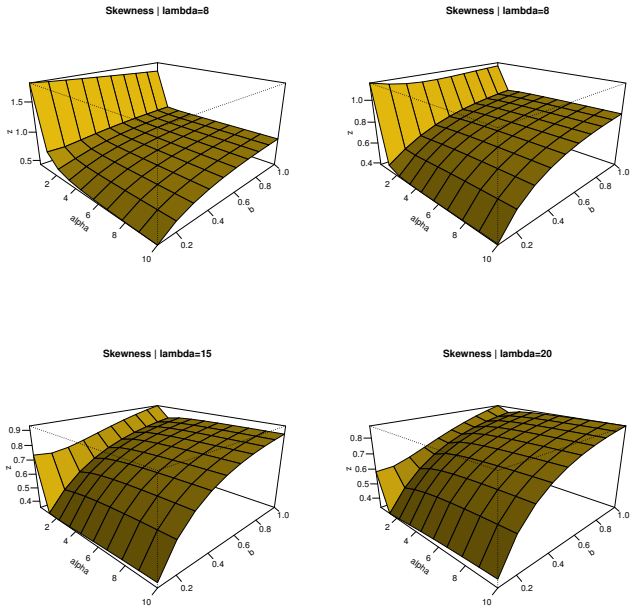

Figure 1. 3D plot of skewness for the EGFrP distribution.

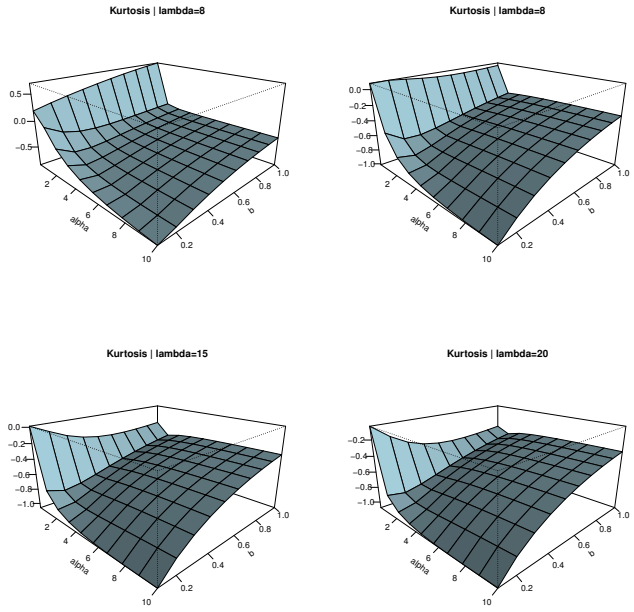

Figure 2. 3D plot of kurtosis for the EGFrP distribution.

4.4. Incomplete moments

The s^{th} incomplete moment, say $\xi_{s,X}(t)$, is given by $\xi_{s,X}(t) = \int_{-\infty}^{t} x^s f(x)\,dx$. Using (7), we obtain

$$\xi_{s,X}(t) = \sum_{\kappa_3=0}^{\infty} \zeta_{\kappa_3} a^s \kappa_3^{*\frac{s}{b}} \gamma\left(1 - \frac{s}{b}, \left(at^{-1}\right)^b\right) |_{b>s}, \tag{16}$$

where

$$\gamma(\tau_1, \tau_2) = \int_0^{\tau_2} t^{\tau_1 - 1} \exp(-t)\,dt = \frac{\tau_2^{\tau_1}}{\tau_1} \left\{{}_1\mathbf{F}_1\left[\tau_1; \tau_1\tau_2 + 1; -\tau_2\right]\right\} = \sum_{\kappa_3=0}^{\infty} \frac{(-1)^{\kappa_3}}{\kappa_3!\,(\tau_1 + \kappa_3)} \tau_2^{\tau_1 + \kappa_3},$$

the function ${}_1\mathbf{F}_1[\cdot,\cdot,\cdot]$ is called the confluent hypergeometric function. The first incomplete moment of the EGFrP model, $\xi_{1,X}(t)$, can be obtained by setting $s = 1$ in (16).

4.5. Probability Weighted Moments (PWMs)

The $(s,r)^{\text{th}}$ PWM of X following the EGFrP model, say $\rho_{s,r}$, is formally defined by $\rho_{s,r,X} = \mathbf{E}\left\{X^s F(X)^r\right\}$. Using equations (5) and (6), we can write

$$f(x)\ F(x)^r = \sum_{\kappa_3=0}^{\infty} w_{\kappa_3} \pi_{\kappa_3^*}(x; a, b),$$

where

$$w_{\kappa_3} = \frac{\alpha\beta}{\mathbf{c}_{[\lambda]}\kappa_3^*} \sum_{w,\kappa_1,\kappa_2=0}^{\infty} \frac{(-1)^{w+\kappa_1+\kappa_2+\kappa_3}}{\kappa_1!\lambda^{-\kappa_1-1}\,(1+w)^{-\kappa_1}} \binom{r}{w} \binom{\beta(\kappa_1+1)-1}{\kappa_2} \binom{\alpha(1+\kappa_2)-1}{\kappa_3}.$$

Then, the $(s,r)^{\text{th}}$ PWM of X can be expressed as

$$\rho_{s,r,X} = \sum_{\kappa_3=0}^{\infty} w_{\kappa_3} a^s \kappa_3^{*\frac{s}{b}} \mathbf{\Gamma}\left(1 - \frac{s}{b}\right) |_{b>s}.$$

4.6. Residual Life and Reversed Residual Life

The n^{th} moment of the residual life, say

$$\tau_{n,X}(t) = \mathbf{E}\left[(X-t)^n\ |_{n=1,2,\ldots}^{X>t}\right].$$

The n^{th} moment of the residual life of X is given by

$$\tau_{n,X}(t) = \frac{1}{1 - F(t)} \int_t^{\infty} (x-t)^n dF(x).$$

Therefore, we have

$$\tau_{n,X}(t) = \frac{1}{1 - F(t)} \sum_{\kappa_3=0}^{\infty} \zeta_{\kappa_3}^* a^n \kappa_3^{*\frac{n}{b}} \mathbf{\Gamma}\left(1 - \frac{n}{b}, \left(at^{-1}\right)^b\right) |_{b>n}, \tag{17}$$

where

$$\zeta_{\kappa_3}^* = \zeta_{\kappa_3} \sum\nolimits_{r=0}^{n} \binom{n}{r} (-t)^{n-r}$$

and

$$\mathbf{\Gamma}(\tau_1, \tau_2) = \mathbf{\Gamma}(\tau_1) - \gamma(\tau_1, \tau_2) = \int_{\tau_2}^{\infty} t^{\tau_1 - 1} \exp(-t)\,dt.$$

The n^{th} moment of the reversed residual life can be expressed as

$$\omega_{n,X}(t) = \mathbf{E}\left[(t-X)^n \mid_{n=1,2,\ldots}^{X\leq t \text{ and } t>0}\right]$$

or as

$$\omega_{n,X}(t) = \frac{1}{F(t)}\int_0^t (t-x)^n dF(x).$$

Then, the n^{th} moment of the reversed residual life of X becomes

$$\omega_{n,X}(t) = \frac{1}{F(t)}\sum_{\kappa_3=0}^{\infty} \zeta_{\kappa_3}^{**} a^n \kappa_3^{*\frac{n}{b}} \gamma\left(1-\frac{n}{b}, \left(at^{-1}\right)^b\right) \mid_{b>n}, \tag{18}$$

where

$$\zeta_{\kappa_3}^{**} = \zeta_{\kappa_3} \sum\nolimits_{r=0}^{n} (-1)^r \binom{n}{r} t^{n-r}.$$

5. Stress strength reliability model

The stress-strength model is the most widely used approach for reliability estimation. This model is used in many applications of physics and engineering such as strength failure and system collapse. In stress-strength modeling,

$$R_{(X_2<X_1)} = \Pr(X_2 < X_1) = \int_0^{\infty} f(x_1) F(x_2)\, dx, \tag{19}$$

is a measure of reliability of the system when it is subjected to random stress X_2 and has strength X_1. The system fails if and only if the applied stress is greater than its strength and the component will function satisfactorily whenever $X_1 > X_2$. $R_{(X_2<X_1)}$ can be considered as a measure of system performance and naturally arise in electrical and electronic systems. Other interpretation can be that, the reliability, say $R_{(X_2<X_1)}$, of the system is the probability that the system is strong enough to overcome the stress imposed on it. Let X_1 and X_2 be two independent positive random variables having EGFrP $(\alpha_1, \beta_1, \lambda_1, a, b)$ and EGFrP $(\alpha_2, \beta_2, \lambda_2, a, b)$ distributions. The reliability $R_{(X_2<X_1)}$ is given by

$$R_{(X_2<X_1)} = \int_0^{\infty} f_1(x;\alpha_1,\beta_1,\lambda_1,a,b) F_2(x;\alpha_2,\beta_2,\lambda_2,a,b) dx.$$

Then, we have

$$R_{(X_2<X_1)} = \sum_{\kappa_5,\kappa_6=0}^{\infty} \Upsilon_{\kappa_5,\kappa_6}, \tag{20}$$

where

$$\begin{aligned}\Upsilon_{\kappa_5,\kappa_6} &= \frac{\alpha_1\alpha_2\beta_1\beta_2(-1)^{\kappa_5+\kappa_6}}{\mathbf{c}_{[\lambda_1]}\mathbf{c}_{[\lambda_2]}} \sum_{\kappa_1,\kappa_2,\kappa_3,\kappa_4=0}^{\infty} \frac{(-1)^{\kappa_1+\kappa_2+\kappa_3+\kappa_4}}{\kappa_1!\kappa_3!\lambda_1^{-\kappa_1-1}\lambda_2^{-\kappa_3-1}(\kappa_6+1)(\kappa_5+\kappa_6+2)} \\ &\times \binom{\beta_1(\kappa_1+1)-1}{\kappa_2}\binom{\beta_2\kappa_3^*-1}{\kappa_4}\binom{\alpha_1(\kappa_2+1)-1}{\kappa_5}\binom{\alpha_2(\kappa_4+1)-1}{\kappa_6}.\end{aligned}$$

6. Estimation

6.1. The maximum likelihood estimation method

Let $X_1, X_2, \ldots, X_n$ be a random sample from the EGFrP model with parameters $\lambda, \alpha, \beta, a$ and b. Let $\underline{\mathbf{\Omega}} = (\alpha, \beta, \lambda, a, b)^{\intercal}$ be a 5×1 parameter vector. For determining the maximum likelihood estimation (MLE) of $\underline{\mathbf{\Omega}}$,

we have the log-likelihood function

$$\begin{aligned}\ell_{(\underline{\mathbf{\Omega}})} &= n\log\alpha + n\log\beta + n\log\lambda - n\log\left[1-\exp(-\lambda)\right] + n\log b + nb\log a \\ &\quad -(b+1)\sum_{i=1}^{n}\log x_i - \sum_{i=1}^{n}\left(ax_i^{-1}\right)^b + (\alpha-1)\sum_{i=1}^{n}\log\left\{1-\varrho\left(x_i|a,b\right)\right\} \\ &\quad +(\beta-1)\sum_{i=1}^{n}\log\left(1-\left\{1-\varrho\left(x_i|a,b\right)\right\}^{\alpha}\right) \\ &\quad -\lambda\sum_{i=1}^{n}\left(1-\left\{1-\varrho\left(x_i|a,b\right)\right\}^{\alpha}\right)^{\beta},\end{aligned}$$

where $\varrho\left(x_i|a,b\right)=\exp\left[-\left(ax_i^{-1}\right)^b\right]$. The components of the score vector

$$\mathbf{U}\left(\underline{\mathbf{\Omega}}\right)=\frac{\partial\ell}{\partial\underline{\mathbf{\Omega}}}=\left(\mathbf{U}_\alpha=\frac{\partial\ell}{\partial\alpha},\mathbf{U}_\beta=\frac{\partial\ell}{\partial\beta},\mathbf{U}_\lambda=\frac{\partial\ell}{\partial\lambda},\mathbf{U}_a=\frac{\partial\ell}{\partial a},\mathbf{U}_b=\frac{\partial\ell}{\partial b}\right)^{\intercal},$$

can be easily derived. It is usually more convenient to use nonlinear optimization methods such as the quasi-Newton algorithm to numerically maximize ℓ. For interval estimation of the parameters, we obtain the 5×5 observed information matrix $\mathbf{J}(\underline{\mathbf{\Omega}})=\{\frac{\partial^2\ell}{\partial r\,\partial s}\}$ (for $r,s=\alpha,\beta,\lambda,a,b$), whose elements can be computed numerically. Under standard regularity conditions when $n\to\infty$, the distribution of $\widehat{\underline{\mathbf{\Omega}}}$ can be approximated by a multivariate normal $N_5(0,J(\widehat{\underline{\mathbf{\Omega}}})^{-1})$ distribution to construct approximate confidence intervals for the parameters. Here, $\mathbf{J}(\widehat{\underline{\mathbf{\Omega}}})$ is the total observed information matrix evaluated at $\widehat{\underline{\mathbf{\Omega}}}$. The method of the re-sampling Boot. can be used for correcting the biases of the MLEs of the model parameters. Good interval estimates may also be obtained using the Boot. percentile method. The elements of $\mathbf{J}(\underline{\mathbf{\Omega}})$ are easily to be derived.

6.2. The Cramér–von Mises estimation (CVME) method

The CVME of the parameter vector $\underline{\mathbf{\Psi}}$ are obtained via minimizing the following expression with respect to θ,a,b and c , where

$$\mathbf{CVM}_{(\underline{\mathbf{\Psi}})}=\frac{1}{12}n^{-1}+\sum_{i=1}^{n}\left[F_{\underline{\mathbf{\Psi}}}\left(x_i\right)-d_{(i,n)}^{[1]}\right]^2,$$

and $d_{(i,n)}^{[1]}=\frac{2i-1}{2n}$, then

$$\mathbf{CVM}_{(\underline{\mathbf{\Psi}})}=\sum_{i=1}^{n}\left[F_{\underline{\mathbf{\Psi}}}\left(x_i\right)-d_{(i,n)}^{[1]}\right]^2.$$

Then, CVME are obtained by as presented by Ibrahim [52] and solving the following non-linear equations

$$\sum_{i=1}^{n}\left\{\frac{1-\tau_{\varrho}}{\mathbf{c}_{[\lambda]}}-d_{(i,n)}^{[1]}\right\}Q_{(\alpha)}(x_i,\underline{\mathbf{\Psi}})=0,\sum_{i=1}^{n}\left\{\frac{1-\tau_{\varrho}}{\mathbf{c}_{[\lambda]}}-d_{(i,n)}^{[1]}\right\}Q_{(\beta)}(x_i,\underline{\mathbf{\Psi}})=0,$$

$$\sum_{i=1}^{n}\left\{\frac{1-\tau_{\varrho}}{\mathbf{c}_{[\lambda]}}-c_{(i,n)}^{[1]}\right\}Q_{(\lambda)}(x_i,\underline{\mathbf{\Psi}})=0,\sum_{i=1}^{n}\left\{\frac{1-\tau_{\varrho}}{\mathbf{c}_{[\lambda]}}-d_{(i,n)}^{[1]}\right\}Q_{(a)}(\lambda,\underline{\mathbf{\Psi}})=0,$$

and

$$\sum_{i=1}^{n}\left\{\frac{1-\tau_{\varrho}}{\mathbf{c}_{[\lambda]}}-d_{(i,n)}^{[1]}\right\}Q_{(b)}(x_i,\underline{\mathbf{\Psi}})=0,$$

where τ_{ϱ}=$\exp\left[-\lambda\left(1-\left\{1-\varrho\left(x_i|a,b\right)\right\}^{\alpha}\right)^{\beta}\right]$, $Q_{(*)}(x_i,\underline{\mathbf{\Psi}})=\partial F_{\underline{\mathbf{\Psi}}}\left(x_i\right)/\partial\left(*\right)$ are the first derivatives of the CDF of PBXIW distribution with respect to α,β,λ,a,b respectively.

6.3. The Boot. estimation method

The broader category of resampling methods encompasses bootstrapping, a technique that employs random sampling with replacement to mimic the original sampling process. Bootstrapping allows for the estimation of various statistical properties, such as bias, variance, confidence intervals, prediction error, and more, providing accuracy assessments for sample estimates. This approach can approximate the sampling distribution of nearly any statistic by leveraging random sampling techniques. A commonly used approximation is the empirical distribution function derived from the observed data. When it is reasonable to assume that a dataset originates from a population with a consistent distribution, bootstrapping involves creating multiple resamples (with replacement) from the observed data, each of the same size as the original dataset. This method is particularly powerful in applications where the sample size is small, as it does not rely on traditional assumptions about the underlying distribution of the data. In general, when sample sizes are less than 40, assuming a normal or t-distribution may not be appropriate. However, bootstrapping performs effectively even with fewer than 40 observations because it relies on resampling rather than distributional assumptions. The technique makes no presuppositions about the shape or nature of the data's distribution, making it highly versatile. The increasing popularity of bootstrapping is largely due to advancements in computing power, as the method requires significant computational resources to repeatedly resample and analyze datasets. Historically, this computational demand limited its practicality, but modern technology has made bootstrapping an accessible and widely-used tool in statistical analysis. By enabling the use of resampling techniques without distributional assumptions, bootstrapping has become an indispensable method for robust statistical inference.

6.4. KE method

The KEs are obtained by minimizing the function

$$K = \max_{1\leq i\leq n}\left\{\frac{i}{n} - F_{\underline{\mathbf{\Psi}}}\left(x_{i:n}\right), F_{\underline{\mathbf{\Psi}}}\left(x_{i:n}\right) - d^{[2]}_{(i,n)}\right\},$$

where

$$d^{[2]}_{(i,n)} = \frac{i-1}{n}.$$

6.5. Anderson–Darling left-tail of the second order (AD2LE)

The AD2LEs are obtained by minimizing

$$\mathbf{AD2LE}\left(\underline{\mathbf{\Psi}}\right) = 2\sum_{i=1}^{n}\log\left[F_{\underline{\mathbf{\Psi}}}\left(x_{i:n}\right)\right] + \frac{1}{n}\sum_{i=1}^{n}\frac{2i-1}{F_{\underline{\mathbf{\Psi}}}\left(x_{i:n}\right)}.$$

Then, the parameter estimates can be obtained by solving the nonlinear equations

$$\begin{aligned}\partial\left[\mathbf{AD2LE}\left(\underline{\mathbf{\Psi}}\right)\right]/\partial\alpha &= 0,\ \partial\left[\mathbf{AD2LE}\left(\underline{\mathbf{\Psi}}\right)\right]/\partial\beta = 0,\\ \partial\left[\mathbf{AD2LE}\left(\underline{\mathbf{\Psi}}\right)\right]/\partial\lambda &= 0,\ \partial\left[\mathbf{AD2LE}\left(\underline{\mathbf{\Psi}}\right)\right]/\partial a = 0\end{aligned}$$

and

$$\partial\left[\mathbf{L.T.}\ \mathbf{ADE}\left(\underline{\mathbf{\Psi}}\right)\right]/\partial b = 0.$$

7. Simulation studies

In this section, we present a comprehensive simulation study designed to evaluate and compare the performance of five estimation methods under varying sample sizes. The primary objective is to assess the accuracy and consistency of these methods in estimating parameters of a given distribution, as measured by the MSE. The simulation is conducted for three different sample sizes: n =50, n =100, and n =200, allowing us to examine how

Table 1: The MSEs for $n = 50$.

Parameters	MLE	CVM	Boot.	KE	AD2LE
$\alpha = 0.9$	0.02354	0.03155	0.01346	0.03950	244.6381
$\beta = 0.9$	0.01504	0.02250	0.08192	0.02199	0.01887
$\lambda = 0.5$	0.24780	0.26775	0.40109	0.29456	160.0155
$a = 1.5$	0.01978	0.02970	0.10252	0.03027	0.02530
$b = 1.5$	0.02551	0.04406	0.15889	0.08287	0.04739
$\alpha = 1.2$	0.02459	0.02944	0.03503	0.03657	1.58083
$\beta = 1.5$	0.04098	0.05481	0.03789	0.05037	0.04981
$\lambda = 0.8$	0.26120	0.26322	0.33283	0.05037	74.40626
$a = 0.9$	0.01524	0.01968	0.01358	0.01803	0.01897
$b = 0.9$	0.01024	0.02266	0.03158	0.03126	0.02798

the performance of each method evolves with increasing data availability. Tables 1, 2, and 3 summarize the MSEs for each method and parameter combination at the respective sample sizes. These results not only highlight the relative performance of the methods but also shed light on their suitability for practical applications where accurate parameter estimation is critical.

Table 1 presents the MSE for five estimation methods for a simulation study with sample size n =50. The MSEs are calculated for different parameter values (α,β,λ,a, b) under two scenarios: (α =0.9, β =0.9, λ=0.5, a =1.5, b =1.5) and (α =1.2, β =1.5, λ=0.8, a =0.9, b =0.9). Overall, the performance of the methods varies significantly across parameters and applications. For the first scenario (α =0.9), Bootstrapping achieves the lowest MSE for α (0.01346) and β (0.08192), but its performance deteriorates for other parameters, particularly λ (0.40109) and b (0.15889). MLE generally performs well, providing consistently low MSEs for most parameters, except for λ (0.24780). CVM shows moderate performance, with slightly higher MSEs than MLE but lower than Bootstrapping for most parameters. The KE method exhibits mixed results, performing reasonably well for β but poorly for others like λ. Notably, AD2LE produces extremely high MSEs for all parameters in this scenario, making it unsuitable. In the second scenario (α =1.2), MLE and CVM remain competitive, with MLE showing slightly better performance overall. Bootstrapping performs well for α and a, but its MSEs increase for other parameters. KE demonstrates reasonable consistency, though not as strong as MLE or CVM. The AD2LE again shows poor performance, with unacceptably high MSEs for most parameters. Based on these results, MLE emerges as the most reliable method across both scenarios due to its consistent performance, followed closely by CVM . Bootstrapping and KE may be suitable for specific parameters but exhibit variability, while AD2LE is not recommended due to its high MSEs. This analysis underscores the importance of selecting an estimation method tailored to the specific parameter and dataset characteristics.Table 2 presents the MSEs for five estimation methods in a simulation study with a larger sample size of n =100. The MSEs are evaluated for different parameter values (α,β,λ,a,b) under two scenarios: (α =0.9, β =0.9, λ=0.5, a =1.5, b =1.5) and (α =1.2, β =1.5, λ=0.8, a =0.9, b =0.9). As expected, the overall MSEs decrease compared to the n =50 case due to the larger sample size, but the relative performance of the methods remains informative. For the first scenario (α =0.9), MLE consistently exhibits the lowest MSEs across all parameters, with particularly strong performance for α (0.01015), β (0.00780), and λ (0.12264). The CVM closely follows MLE, showing slightly higher but still competitive MSEs. Bootstrapping performs well for some parameters (e.g., α and a) but struggles with others, notably λ (0.46956) and b (0.02766). The KE method demonstrates moderate performance, with MSEs generally lying between those of MLE/CVM and Bootstrapping. The AD2LE, however, continues to exhibit unacceptably high MSEs for most parameters, especially λ (6.4134) and b (0.02029). In the second scenario (α =1.2), MLE again stands out as the most reliable method, maintaining low MSEs across all parameters. CVM performs similarly but shows slightly higher variability in certain cases (like α and λ). Bootstrapping's performance improves for some parameters (e.g., α and a) but remains inconsistent for others. The KE method offers reasonable results, though it is outperformed by MLE and CVM in

Table 2: The MSEs for $n = 100$.

Parameters	MLE	CVM	Boot.	KE	AD2LE
$\alpha = 0.9$	0.01015	0.01352	0.01622	0.01726	24.7397
$\beta = 0.9$	0.00780	0.00949	0.05246	0.01013	0.00939
$\lambda = 0.5$	0.12264	0.12032	0.46956	0.13699	6.4134
$a = 1.5$	0.01038	0.01283	0.06501	0.01408	0.01261
$b = 1.5$	0.01269	0.02157	0.02766	0.04135	0.02029
$\alpha = 1.2$	0.01223	0.0428	0.01484	0.01637	0.13954
$\beta = 1.5$	0.02035	0.02516	0.02924	0.02618	0.02571
$\lambda = 0.8$	0.12570	0.12808	0.14916	0.13971	1.18195
$a = 0.9$	0.00755	0.00907	0.00985	0.00937	0.00982
$b = 0.9$	0.00514	0.01148	0.04153	0.01490	0.01239

most cases. AD2LE, despite reduced MSEs compared to n =50, still produces relatively high errors, making it unsuitable for practical use. Based on these findings, MLE is the most robust and consistent method across both scenarios, followed closely by CVM . Bootstrapping and KE may be viable alternatives for specific parameters but exhibit more variability. AD2LE is not recommended due to its persistently high MSEs, even with the increased sample size. This analysis highlights the importance of selecting an estimation method that balances accuracy and consistency, especially as sample sizes grow.

Table 3 presents the MSEs for the five estimation methods in a simulation study with a sample size of n =200. The MSEs are evaluated for different parameter values (α,β,λ,a,b) under two scenarios: (α =0.9, β =0.9, λ=0.5,a =1.5, b =1.5) and (α =1.2, β =1.5, λ=0.8, a =0.9, b =0.9). With the increased sample size, the overall MSEs decrease compared to smaller sample sizes (n =50 and n =100), allowing for a clearer comparison of the methods' relative performance. For the first scenario (α =0.9), MLE consistently exhibits the lowest MSEs across all parameters, such as α (0.00527), β (0.00366), and λ (0.05939). The CVM closely follows MLE, with slightly higher but still competitive MSEs. Bootstrapping performs well for some parameters (e.g., β and a) but shows higher variability for others, particularly λ (0.08821) and b (0.01421). The KE method demonstrates moderate performance, generally lying between MLE and Bootstrapping. AD2LE, however, continues to exhibit significantly higher MSEs, especially for λ (0.20561) and b (0.02029), making it unsuitable for practical use. In the second scenario (α =1.2), MLE again stands out as the most reliable method, maintaining low MSEs across all parameters. The CVM performs similarly but shows slightly higher errors for certain parameters (e.g., α and λ). Bootstrapping's performance improves for some parameters (e.g., α and β) but remains inconsistent for others. The KE method offers reasonable results but is outperformed by MLE and CVM in most cases. The AD2LE, despite reduced MSEs compared to smaller sample sizes, still produces relatively high errors, particularly for λ (0.44389). Based on these findings, the MLE is the most robust and consistent method across both scenarios, followed closely by CVM . Bootstrapping and KE may be viable alternatives for specific parameters but exhibit more variability. The AD2LE is not recommended due to its persistently high MSEs, even with the larger sample size. This analysis underscores the importance of selecting an estimation method that balances accuracy and consistency, especially as sample sizes increase, ensuring reliable parameter estimation.

Finally, Table 4 presents the MSEs for different parameter estimates obtained using various estimation methods, including MLE, CVM, Bootstrap,KE, and AD2LE, based on simulated data where $n = 500$. A comparative analysis of the results reveals that MLE and CVM consistently yield lower MSEs across most parameters, indicating their reliability in providing more stable estimates. In contrast, the Bootstrap method exhibits higher MSEs, particularly for the parameter λ, suggesting that it introduces greater variability in estimation. KE and AD2LE display fluctuating performance, with AD2LE producing notably large errors for specific parameters, highlighting its inconsistency. Among all parameters, λ appears to be the most challenging to estimate accurately, as it consistently results in higher MSE values across all methods. These findings suggest that MLE and CVM

Table 3: The MSEs for $n = 200$.

Parameters	MLE	CVM	Boot.	KE	AD2LE
$\alpha = 0.9$	0.00527	0.00700	0.01288	0.00767	0.06007
$\beta = 0.9$	0.00366	0.00481	0.00343	0.00511	0.00939
$\lambda = 0.5$	0.05939	0.06295	0.08821	0.06561	0.20561
$a = 1.5$	0.00488	0.00655	0.00463	0.00705	0.01261
$b = 1.5$	0.00597	0.01092	0.01421	0.02122	0.02029
$\alpha = 1.2$	0.00571	0.00707	0.00702	0.00729	0.05109
$\beta = 1.5$	0.00891	0.01202	0.00913	0.01284	0.01277
$\lambda = 0.8$	0.05918	0.06333	0.07638	0.06548	0.44389
$a = 0.9$	0.00331	0.00434	0.00334	0.00459	0.00489
$b = 0.9$	0.00255	0.00533	0.00424	0.00777	0.00528

Table 4: The MSEs for $n = 500$.

Parameters	MLE	CVM	Bootstrap	KE	AD2LE
$\alpha = 0.9$	0.00221	0.00263	0.00384	0.00287	0.01667
$\beta = 0.9$	0.00137	0.00183	0.00257	0.00197	0.00225
$\lambda = 0.5$	0.02493	0.02392	0.04793	0.02522	0.08186
$a = 1.5$	0.00182	0.00250	0.00355	0.00271	0.00302
$b = 1.5$	0.00201	0.00439	0.00680	0.00797	0.00440
$\alpha = 1.2$	0.00335	0.00277	0.00534	0.00282	0.01213
$\beta = 1.5$	0.00339	0.00486	0.00779	0.00498	0.00564
$\lambda = 0.8$	0.02305	0.02527	0.06056	0.02558	0.08101
$a = 0.9$	0.00126	0.00176	0.00292	0.00178	0.00216
$b = 0.9$	0.00092	0.00237	0.00315	0.00299	0.00234

are the most effective estimation techniques in terms of minimizing MSE, whereas Bootstrap and AD2LE may introduce additional variability and uncertainty in parameter estimation.

8. Applications for comparing methods

This Section compares the MLE, CVME, Bootstrapping, KE method, and AD2LEs methods for fitting distributions to real datasets. Two datasets are analyzed: 100 observations of carbon fiber breaking stress (Nichols and Padgett [70]) ((0.92, 0.928, 0.997, 0.9971, 1.061, 1.117, 1.162, 1.183, 1.187, 1.192, 1.196, 1.213, 1.215, 1.2199, 1.22, 1.224, 1.225, 1.228, 1.237, 1.24, 1.244, 1.259, 1.261, 1.263, 1.276, 1.31, 1.321, 1.329, 1.331, 1.337, 1.351, 1.359, 1.388, 1.408, 1.449, 1.4497, 1.45, 1.459, 1.471, 1.475, 1.477, 1.48, 1.489, 1.501, 1.507, 1.515, 1.53, 1.5304, 1.533, 1.544, 1.5443, 1.552, 1.556, 1.562, 1.566, 1.585, 1.586, 1.599, 1.602, 1.614, 1.616, 1.617, 1.628, 1.684, 1.711, 1.718, 1.733, 1.738, 1.743, 1.759, 1.777, 1.794, 1.799, 1.806, 1.814, 1.816, 1.828, 1.83, 1.884, 1.892, 1.944, 1.972, 1.984, 1.987, 2.02, 2.0304, 2.029, 2.035, 2.037, 2.043, 2.046, 2.059, 2.111, 2.165, 2.686, 2.778, 2.972, 3.504, 3.863, 5.306)) and 63 observations of glass fiber strengths (Smith and Naylor [88]) (1.014, 1.081, 1.082, 1.185, 1.223, 1.248, 1.267, 1.271, 1.272, 1.275, 1.276, 1.278, 1.286, 1.288, 1.292, 1.304, 1.306, 1.355, 1.361, 1.364, 1.379, 1.409, 1.426, 1.459, 1.46, 1.476, 1.481, 1.484, 1.501, 1.506, 1.524, 1.526, 1.535, 1.541, 1.568, 1.579, 1.581, 1.591, 1.593, 1.602, 1.666, 1.67, 1.684, 1.691, 1.704, 1.731, 1.735, 1.747, 1.748, 1.757, 1.800, 1.806, 1.867, 1.876, 1.878, 1.91, 1.916, 1.972, 2.012, 2.456, 2.592, 3.197, 4.121). The performance of these methods is evaluated using the Anderson–Darling (AD) and Cramér–von Mises (CvM) criteria, which assess goodness-of-fit. MLE is found to be efficient but may underperform in small samples, while CVME provides robust results across datasets. For

Table 5: Comparing methods under the carbon fiber breaking stress data.

	$\widehat{\alpha}$	$\widehat{\beta}$	$\widehat{\lambda}$	$\widehat{a}$	$\widehat{b}$	CvM	AD
MLE	2.121	1.855	0.787	1.541	2.626	0.079	0.595
CVM	6.377	6.960	−1.758	1.526	1.418	0.080	0.674
KE	2.442	1.924	−0.481	0.425	0.206	0.192	1.463
Bootst.	2.265	1.461	1.483	1.778	2.391	0.074	0.556
AD2LE	4.747	1.452	0.973	2.227	1.844	0.079	0.659

Table 6: Comparing methods under the strengths data.

	$\widehat{\alpha}$	$\widehat{\beta}$	$\widehat{\lambda}$	$\widehat{a}$	$\widehat{b}$	CvM	AD
MLE	43.673	0.215	-4.882	3.975	1.494	7.914	47.765
CVM	9.535	5.122	-3.407	1.763	1.763	0.729	3.980
KE	5.744	4.680	-1.795	0.865	0.00004	0.701	3.830
Bootst.	82.718	0.357	-4.485	4.091	1.585	0.203	1.095
AD2LE	18.511	0.211	-4.252	4.004	1.326	0.428	2.347

more extreme reliability data and related applications see Minkah et al. [69], Yousof et al. [91], Shehata et al. [83], Alizadeh et al. ([26]; [27]). In fact, in the past five years, researchers have become increasingly interested in processing reliability data using probability families and probability distributions, for example see [7], [73], [74], [75], [84], [98], [100], [101], [102], [9], [17], [36], [30], [71], [19], [20], [21], [43], [44], [90], [45], [50] and [51].

Table 5 presents a comparative analysis of five estimation methods for fitting the carbon fiber breaking stress dataset. Among the methods, Bootstrapping emerges as the most effective, achieving the smallest CvM =0.074 and AD=0.556. This indicates its superior ability to capture both the central tendency and the tails of the distribution. While MLE and AD2LE show comparable CvM values (0.079), their higher AD values (0.595 and 0.659, respectively) suggest they are less adept at modeling the tails. Conversely, the KE method performs poorly, with significantly larger CvM =0.192 and AD =1.463, highlighting its unsuitability for this dataset. Thus, Bootstrapping is recommended as the optimal method for estimating parameters in the context of carbon fiber breaking stress data.

Table 6 evaluates the performance of five estimation methods using the CvM and AD criteria for the glass fiber strengths dataset. In this case, the AD2LE method outperforms the others, yielding the smallest CvM =0.428 and AD=2.347, indicating its strong capability to model both the overall distribution and its tails. Bootstrapping ranks second with CvM=0.203 and AD =1.095, demonstrating good but not optimal performance. The KE and CVM methods show moderate results, with similar CvM and AD values CvM ≈0.701, AD≈3.830), suggesting they provide reasonable fits but are less robust than AD2LE. Notably, MLE performs exceptionally poorly, with extremely high CvM=7.914 and AD =47.765, likely due to issues with parameter estimation or model misspecification. Therefore, AD2LE is recommended as the most reliable method for analyzing the glass fiber strengths dataset, particularly when tail behavior is critical.

9. Applications for comparing models

The statistical analysis of the first dataset reveals that the mean (1.6578) is higher than the median (1.5442), indicating a right-skewed distribution, where larger values pull the mean upwards. The mode (0.92), being significantly lower than both the mean and median, further confirms the asymmetry of the data. The standard deviation (0.5994) suggests considerable variation, highlighting a wide spread of values. The high skewness (3.1824) confirms that the dataset is strongly right-skewed, with extreme values such as 3.863 and 5.306 contributing to the long right tail. Moreover, the kurtosis value (14.4236) indicates a leptokurtic distribution, meaning the dataset has heavy tails and a sharp peak, emphasizing the presence of significant outliers. This

suggests that the data is not normally distributed and contains extreme values that could heavily influence mean-based interpretations. Given this, using robust statistical techniques or log transformation may be beneficial when analyzing or modeling this dataset, as standard methods may be overly sensitive to the presence of extreme values. However, the statistical analysis of the second dataset reveals that the mean (1.6156) is higher than the median (1.526), suggesting a right-skewed distribution, where larger values influence the mean. The mode (1.014) is the most frequently occurring value and is significantly lower than both the mean and median, reinforcing the skewness of the data. The standard deviation (0.4818) indicates moderate variability within the dataset. The high skewness (2.9397) confirms that the dataset is strongly right-skewed, with extreme values such as 3.197 and 4.121 pulling the distribution to the right. Additionally, the kurtosis (11.4942) suggests a leptokurtic distribution, characterized by heavy tails and a pronounced peak, implying the presence of significant outliers. Given this distribution, standard statistical techniques might be sensitive to extreme values, and robust methods or transformations may be necessary for accurate data modeling and analysis. For more relevant data sets see [63], [64], [65], [66] [67] and [68].

This section presents two practical applications of the EGFrP distribution using real datasets, aiming to compare its performance and goodness-of-fit with several well-established Fréchet-based distributions, including the Weibull Fréchet (WFr) proposed by Afify et al. [22], which combines the Weibull and Fréchet models for enhanced flexibility in heavy-tailed data; the Exponentiated Fréchet (EFr) introduced by Nadarajah and Kotz [60], extending the Fréchet distribution with an exponentiation parameter to capture diverse data shapes; the Kumaraswamy Fréchet (KumFr), integrating the Kumaraswamy family for greater adaptability to bounded and skewed datasets; the Beta Fréchet (BFr) presented by Barreto-Souza et al. [32], combining the beta family with the Fréchet model for a wide range of tail behaviors; the Transmuted Fréchet (TFr), introducing a transmutation parameter to modify the baseline Fréchet distribution for better fitting of complex patterns; the Gamma Extended Fréchet (GEFr) introduced by Silva et al. [82], incorporating a gamma component to improve modeling of extreme values; the Marshall-Olkin Fréchet (MOFr), utilizing the Marshall-Olkin extension for robust handling of survival and reliability data; and the classical Fréchet (Fr) distribution as a benchmark for comparison. Through these comparisons, we aim to demonstrate the EGFrP distribution's superior flexibility, where (for $x > 0$):

WFr:

$$\begin{aligned} f(x;\alpha,\beta,a,b) &= ab\beta\alpha^{\beta}x^{-(\beta+1)}\exp\left[-b\left(\alpha x^{-1}\right)^{\beta}\right] \\ &\quad\times\left\{1-\exp\left[-\left(\alpha x^{-1}\right)^{\beta}\right]\right\}^{-(b+1)} \\ &\quad\times\exp\left\{-a\left[\frac{\exp\left[-\left(\alpha x^{-1}\right)^{\beta}\right]}{1-\exp\left[-\left(\alpha x^{-1}\right)^{\beta}\right]}\right]^{b}\right\}; \end{aligned}$$

KumFr:

$$f(x;\alpha,\beta,a,b) = ab\beta\alpha^{\beta}\,x^{-(\beta+1)}\,\exp\left[-a\left(\alpha x^{-1}\right)^{\beta}\right]\left\{1-\exp\left[-a\left(\alpha x^{-1}\right)^{\beta}\right]\right\}^{b-1};$$

EFr:

$$f(x;\alpha,\beta,a) = a\beta\alpha^{\beta}\,x^{-(\beta+1)}\,\exp\left[-\left(\alpha x^{-1}\right)^{\beta}\right]\,\left\{1-\exp\left[-\left(\alpha x^{-1}\right)^{\beta}\right]\right\}^{a-1};$$

BFr:

$$f(x;\alpha,\beta,a,b) = \frac{\beta\alpha^{\beta}}{B\left(a,b\right)}\,x^{-(\beta+1)}\,\exp\left[-a\left(\alpha x^{-1}\right)^{\beta}\right]\,\left\{1-\exp\left[-\left(\alpha x^{-1}\right)^{\beta}\right]\right\}^{b-1};$$

GEFr:

$$\begin{aligned} f(x;\alpha,\beta,a,b) &= \frac{a\beta\alpha^{\beta}}{\mathbf{\Gamma}(b)}\, x^{-(\beta+1)}\, \exp\left[-\left(\alpha x^{-1}\right)^{\beta}\right] \\ &\quad \times \left\{1-\exp\left[-\left(\alpha x^{-1}\right)^{\beta}\right]\right\}^{a-1} \\ &\quad \times \left\{-\log\left\{1-\exp\left[-\left(\alpha x^{-1}\right)^{\beta}\right]\right\}^{a}\right\}^{b-1}; \end{aligned}$$

TFr:

$$f(x;\alpha,\beta,a) = \beta\alpha^{\beta}x^{-(\beta+1)}\, \exp\left[-\left(\alpha x^{-1}\right)^{\beta}\right]\left\{(a+1)-2a\exp\left[-\left(\alpha x^{-1}\right)^{\beta}\right]\right\} \mid (|a|\leq 1);$$

MOFr:

$$f(x;\alpha,\beta,a) = a\beta\alpha^{\beta}\, x^{-(\beta+1)}\, \exp\left[-\left(\alpha x^{-1}\right)^{\beta}\right]\left\{a+(1-a)\exp\left[-\left(\alpha x^{-1}\right)^{\beta}\right]\right\}^{-2}.$$

The unknown parameters of the above PDFs are all positive real numbers except for the TFr distribution. In order to compare the distributions, we consider the following criteria: the $-2\widehat{\ell}$ (Maximized Log-Likelihood), AI_C (Akaike Information Criterion), CAI_C (Consistent Akaike Information Criterion), BI_C (Bayesian information criterion) and HQI_C (Hannan-Quinn Information Criterion). These statistics are given by

$$\begin{aligned} \mathrm{AI}_C &= -2\widehat{\ell_{(\underline{\mathbf{\Omega}})}} + 2\kappa, \\ \mathrm{BI}_C &= -2\widehat{\ell_{(\underline{\mathbf{\Omega}})}} + \kappa\log(n), \\ \mathrm{HQI}_C &= -2\widehat{\ell_{(\underline{\mathbf{\Omega}})}} + 2\kappa\log[\log(n)] \end{aligned}$$

and

$$\mathrm{CAI}_C = -2\widehat{\ell_{(\underline{\mathbf{\Omega}})}} + 2\kappa n/(n-\kappa-1),$$

where $\widehat{\ell_{(\underline{\mathbf{\Omega}})}}$ denotes the log-likelihood function evaluated at the MLEs, κ is the number of model parameters and n is the sample size. In evaluating the best-fit model for the given datasets, the selection is based on choosing the model that yields the minimum values for relevant statistical measures, and all computations are performed using the R programming environment. An essential graphical tool in this process is the Total Time on Test (TTT) plot, which serves as a diagnostic method to assess whether the data aligns with a specific distribution, as outlined by Aarset [1]. According to Aarset's findings, the hazard rate function (HRF) exhibits distinct characteristics depending on the shape of the TTT plot: a straight diagonal indicates a constant HRF, a concave plot suggests an increasing HRF, while a convex plot implies a decreasing HRF. Furthermore, if the TTT plot initially displays convexity followed by concavity, the HRF takes on a U-shaped or bathtub form; otherwise, it is unimodal. To visualize the data, Figure 3 provides quantile-quantile (QQ) plots in the first row and box plots in the second row. Additionally, Figure 4 presents the TTT plots in the first row and nonparametric Kernel Density Estimation (KDE) plots in the second row. Figurer 5 presents the estimated PDF, Probability-Probability (P-P) plot, estimated CDF and Kaplan-Meier survival plot for 1^{st} data set. Figurer 6 presents the estimated PDF, P-P plot, estimated CDF and Kaplan-Meier survival plot for 2^{nd} data set. Based on Figures 5 and 6, the empirical HRFs of both datasets are determined to be monotonically increasing. Table 7 presents the $-2\widehat{\ell_{(\underline{\mathbf{\Omega}})}}$, AI_C, BI_C, HQI_C and CAI_C for 1^{st} data. Table 8 shows the MLEs and their standard errors (in parentheses) for 1^{st} data. Table 9 presents the $-2\widehat{\ell_{(\underline{\mathbf{\Omega}})}}$, AI_C, BI_C, HQI_C and CAI_C for 2^{nd} data. Table 10 shows the MLEs and their standard errors (in parentheses) for 2^{nd} data. For more real data sets for checking the applicability see [72], [38], [62], [8], [33], [11], [56],[18], [34], [6], [40],[3], [16] and [48].

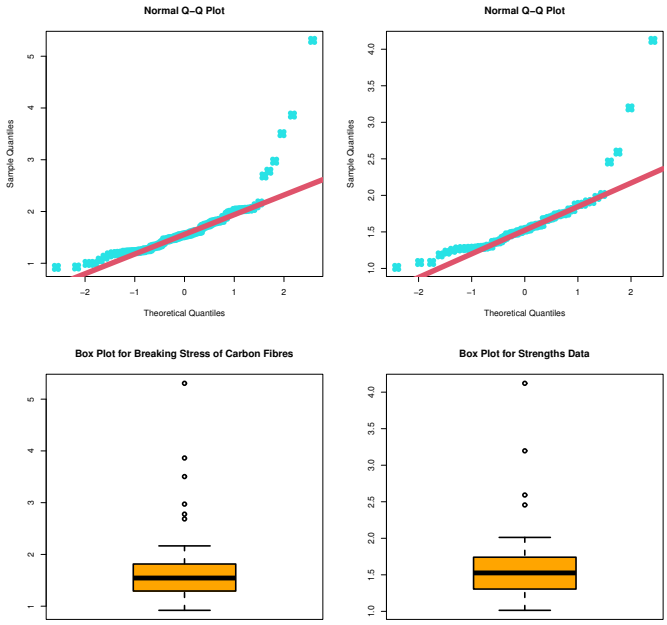

Figure 3. The QQ plots (first row) and box plots (second row).

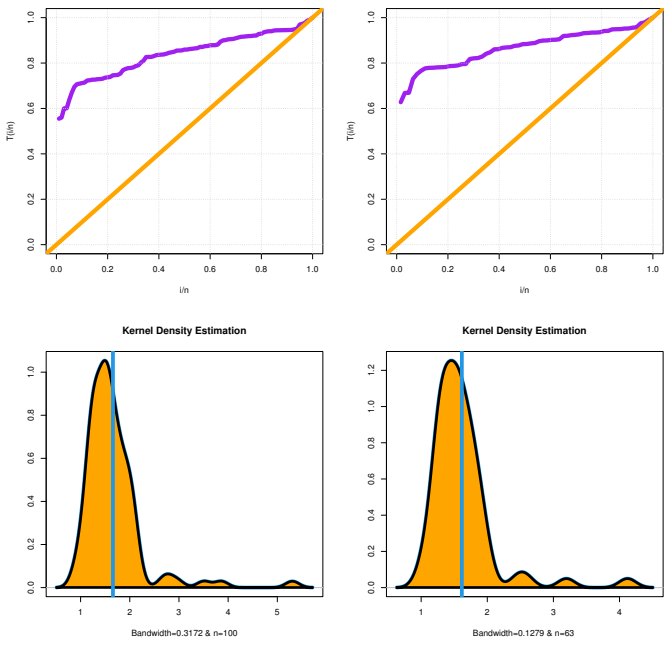

Figure 4. The TTT plots (first row) and KDE plots (second row)

Table 7: $-2\widehat{\ell_{(\underline{\boldsymbol{\Omega}})}}$, AI_C, BI_C, HQI_C and CAI_C for 1^{st} data.

Model	Goodness of fit criteria				
	$-2\widehat{\ell_{(\underline{\boldsymbol{\Omega}})}}$	AI_C	BI_C	HQI_C	CAI_C
EGFrP	**105.4**	**115.44**	**128.46**	**120.71**	**116.08**
WFr	286.5	294.50	304.90	298.70	294.90
EFr	289.7	295.70	303.50	298.90	296.00
KumFr	289.1	297.10	307.50	301.30	297.50
BFr	303.1	311.10	321.60	315.40	311.60
GEFr	304	312.0	332.40	316.20	312.40
Fr	344.3	348.30	353.50	350.40	348.40
TFr	344.5	350.50	358.30	353.60	350.70
MOFr	345.3	351.30	359.10	354.50	351.60

Table 8: MLEs and their standard errors (in parentheses) for 1^{st} data

Model	Estimates				
EGFrP$(\alpha,\beta,\lambda,a,b)$	1.29	1.204	-1.368	1.291	4.221
	(0.000)	(1.059)	(0.000)	(0.001)	(0.002)
WFr(α,β,a,b)	2.2231	0.355	6.9721	4.9179	
	(11.409)	(0.411)	(113.811)	(3.756)	
KumFr(α,β,a,b)	2.0556	0.4654	6.2815	224.18	
	(0.071)	(0.007)	(0.063)	(0.164)	
BFr(α,β,a,b)	1.6097	0.4046	22.0143	29.762	
	(2.498)	(0.108)	(21.432)	(17.48)	
GEFr(α,β,a,b)	1.3692	0.4776	27.6452	17.458	
	(2.017)	(0.133)	(14.136)	(14.82)	
EFr(α,β,a)	69.1489	0.5019	145.328		
	(57.349)	(0.08)	(122.924)		
TFr(α,β,a)	1.9315	1.7435	0.0819		
	(0.097)	(0.076)	(0.198)		
MOFr(α,β,a)	2.3066	1.5796	0.599		
	(0.498)	(0.16)	(0.309)		
Fr(α,β)	1.8705	1.777			
	(0.112)	(0.113)			

Table 9: $-2\widehat{\ell_{(\underline{\boldsymbol{\Omega}})}}$, AI_C, BI_C, HQI_C and CAI_C for 2^{nd} data.

Model	Measures				
	$-2\widehat{\ell_{(\underline{\boldsymbol{\Omega}})}}$	AI_C	BI_C	HQI_C	CAI_C
EGFrP	**39.16**	**49.16**	**58.07**	**52.37**	**50.20**
BFr	60.60	68.60	77.20	72.00	69.30
GEFr	61.60	69.60	78.10	72.90	70.30
Fr	93.70	97.70	102.00	99.40	97.9
TFr	94.10	100.10	106.50	102.60	100.5
MOFr	95.70	101.70	108.20	104.20	102.1

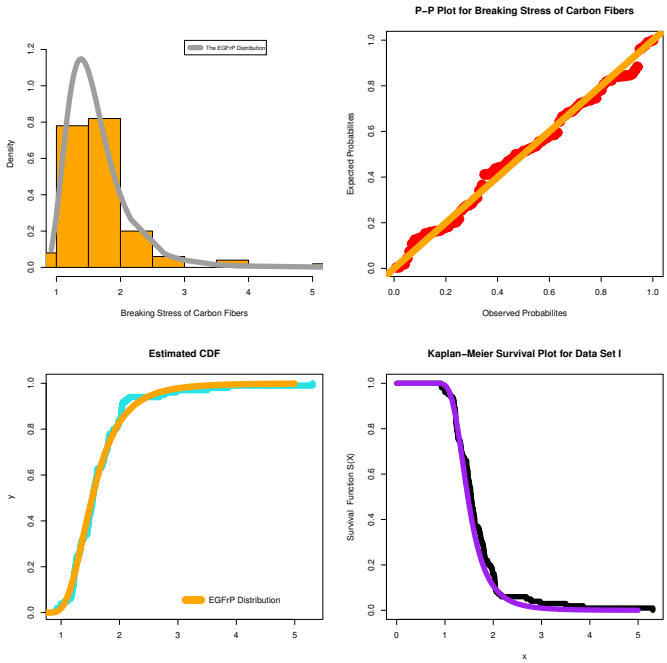

Figure 5. Estimated PDF, P-P plot, estimated CDF and Kaplan-Meier survival plot for 1^{st} data set.

Table 10: MLEs and their standard errors for 2^{nd} data.

Model	Estimates				
EGFrP$(\alpha, \beta, \lambda, a, b)$	0.743	1.88	-3.54	1.05	8.16
	(0.779)	(1.81)	(2.8)	(0.191)	(7.49)
BFr(α, β, a, b)	2.0518	0.6466	15.0756	36.9397	
	(0.986)	(0.163)	(12.057)	(22.649)	
GEFr(α, β, a, b)	1.6625	0.7421	32.112	13.269	
	(0.952)	(0.197)	(17.397)	(9.967)	
TFr(α, β, a)	1.3068	2.7898	0.1298		
	(0.034)	(0.165)	(0.208)		
MOFr(α, β, a)	1.5441	2.3876	0.4816		
	(0.226)	(0.253)	(0.252)		
Fr(α, β)	1.264	2.888			
	(0.059)	(0.234)			

10. Hill estimator under the breaking stress of carbon fibers

The Hill estimator as presented on (11) can provide a robust nonparametric method for estimating the tail index (TIx) of heavy-tailed distributions, which is particularly valuable in analyzing the breaking stress of carbon fibers where extreme values play a critical role in assessing material reliability. Using the breaking stress of carbon fibers data, consisting of $n = 63$ observations, the data was first sorted in descending order to isolate the largest values that dominate the tail behavior. By selecting $n_s = 63$, representing the top 10 largest observations, logarithmic ratios of these values relative to the 10^{th} largest observation were computed, yielding a mean value $Z \approx 1.215$. The inverse of this mean

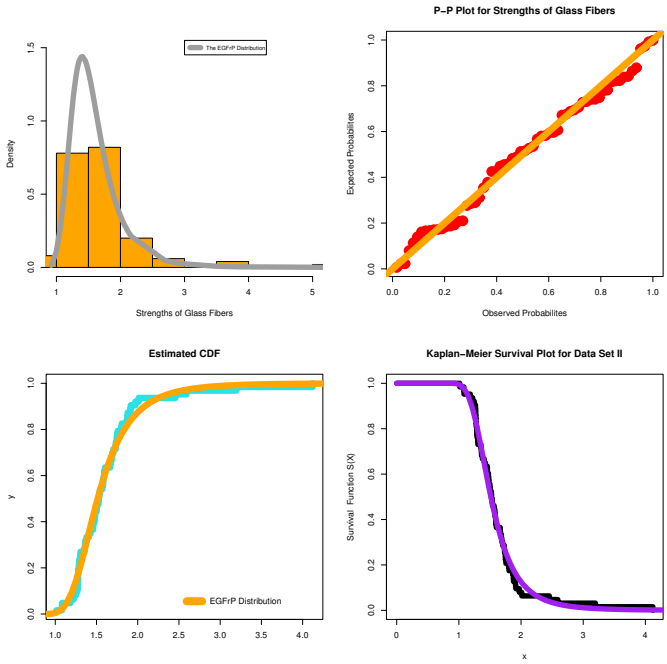

Figure 6. Estimated PDF, P-P plot, estimated CDF and Kaplan-Meier survival plot for 2^{nd} data set.

$$\widehat{\text{TIx}}_{\text{Hill}} = \overline{Z}^{-1} \approx 0.823,$$

A tail index of approximately 0.823 indicates that the breaking stress distribution exhibits very heavy tails. This suggests a higher probability of extreme breaking stress values compared to light-tailed distributions like the normal distribution. Such heavy-tailed behavior is critical in reliability analysis, as it implies a greater likelihood of catastrophic failure under high stress conditions. The Hill estimator's focus on extreme values ensures that this heavy-tailed nature is accurately captured, providing valuable insights for designing safe and reliable structures utilizing carbon fibers. The Hill plot, presented in Figure 6 , provides a visual representation of the Hill estimator's behavior as a function of the number of top-order statistics ($n = 63$) used in the estimation process. This plot is crucial for assessing the stability of the tail index estimate (TIx Hill) across varying values of n. In the context of the breaking stress of carbon fibers, the Hill plot helps identify an optimal range of n where the estimated tail index stabilizes, indicating reliable convergence to a consistent value. A stable region in the Hill plot ensures that the tail index estimate is not unduly influenced by the choice of n, which is particularly important given the variability and potential heavy-tailed nature of the breaking stress data.

Complementing the Hill plot, the stability plot in Figure 8 offers additional insight into the robustness of the tail index estimation. This plot typically displays the logarithm of the Hill estimates against the logarithm of n, providing a clearer visualization of the asymptotic behavior of the tail index. For the breaking stress of carbon fibers, the stability plot confirms the presence of heavy tails by revealing whether the log-log relationship follows a linear trend, which is indicative of a power-law decay in the survival function. Together, these two plots serve as essential diagnostic tools for validating the reliability of the Hill estimator. By examining both the Hill plot and the stability plot, researchers can ensure that the estimated tail index accurately reflects the true tail behavior of the breaking stress distribution, thereby enabling more informed decisions regarding material reliability, risk assessment, and structural design in engineering applications involving carbon fibers.

This tail index suggests that the breaking stress distribution exhibits very heavy tails, implying a significantly higher probability of extreme stress values compared to light-tailed distributions like the normal distribution.

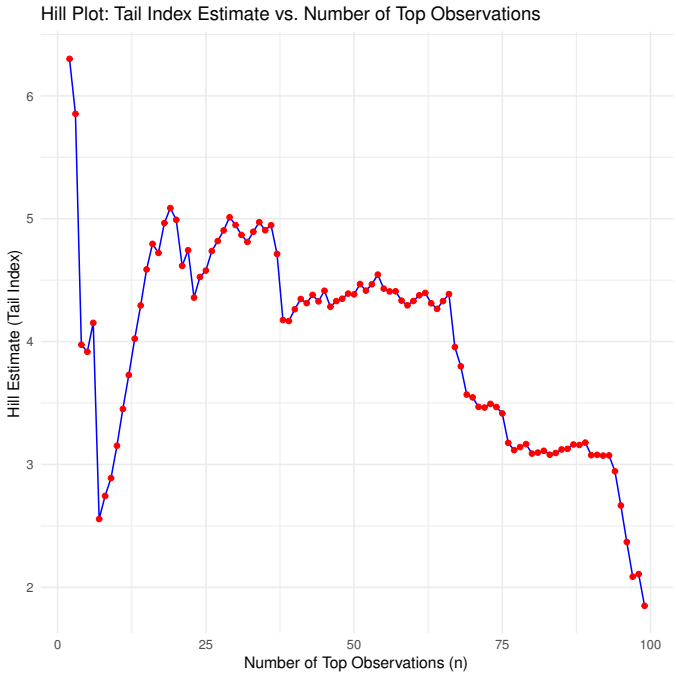

Figure 7. Hill plot for the breaking stress of carbon fibers.

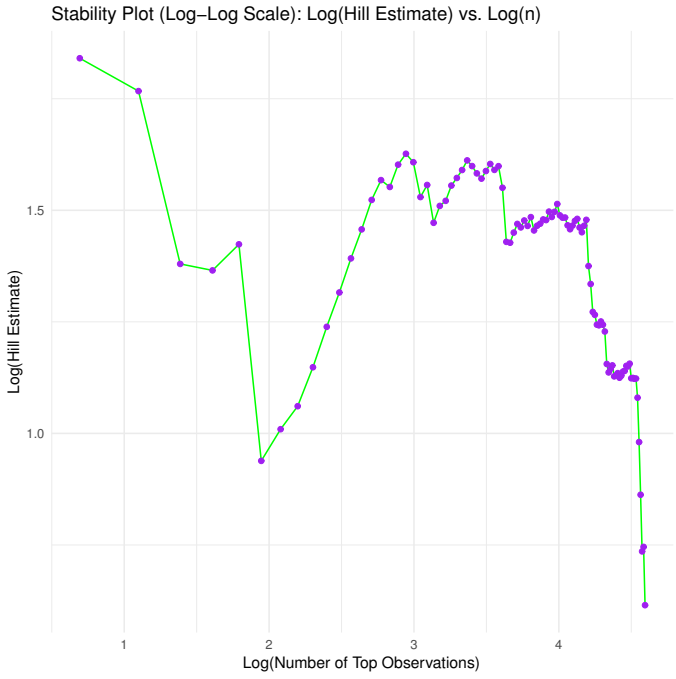

Figure 8. Stability plot for the breaking stress of carbon fibers.

Such behavior is essential for reliability analysis, as it highlights the potential for catastrophic failures under extreme stress conditions, necessitating conservative safety margins in material design. These findings significantly contribute to the understanding of material reliability in structural applications, providing engineers with robust statistical tools for evaluating risk, designing failure-resistant materials, and ensuring the safety of carbon fiber-based components. Please let us know if further refinements are needed.

11. Case Study: Reliability analysis of composite materials for aerospace applications

Reliability analysis is crucial in engineering, medicine, and risk assessment, ensuring structures perform under varying stresses. Strength-stress reliability analysis assesses whether a system's strength surpasses the applied stress. Ibrahim et al. [49] developed a novel test for right-censored validity under a new Chen extension. Yousof et al. [97] proposed a modified Bagdonavičius-Nikulin test for censored distributions. Salem et al. [81] introduced a Lomax extension for left-skewed reliability data, and Saber et al. [78] examined remained stress-strength models under the generalized exponential distribution, later extending it to multicomponent stress-strength models. Rasekhi et al. [105] estimated multicomponent stress-strength reliability under the Topp-Leone distribution via Bayesian and non-Bayesian methods. Rasekhi et al. [77] compared Bayesian and classical inference in multicomponent stress-strength reliability under the generalized logistic model, highlighting Bayesian advantages. Bandar et al. [31] extended the Reduced-Kies family for reliability engineering data. Yousof et al. [105] explored a new discrete generator for reliability, medicine, and biology. Abiad et al. [2] studied copula types for reliability applications with a new Fisk probability model. These studies enhance reliability assessments in aerospace, engineering, medicine, and finance. See also [28], [5], [47] and [79] for more relevant applications.

Here are two hypothetical datasets representing breaking strength (X_1) of the carbon fiber-reinforced polymer (CFRP) and applied operational stress (X_2) in megapascals (MPa), based on realistic engineering scenarios. These values are inspired by existing literature on CFRP materials used in aerospace structures. Table 11 presents the strength (X_1) and applied stress (X_2) data in megapascals (MPa) for 15 hypothetical aerospace structure samples. The strength values represent the maximum load-bearing capacity of the materials used in these structures before failure, while the stress values indicate the operational loads they experience during service. Examining the data, the strength of the structures varies between 1785 MPa (sample 3) and 1,930 MPa (sample 14), while the applied stress ranges from 1185 MPa (sample 3) to 1330 MPa (sample 14). The difference between strength and stress determines the reliability margin, with larger differences indicating safer structural performance. In general, for all samples, the strength (X_1) exceeds the stress (X_2), implying that the structures can sustain their applied loads without immediate risk of failure. However, the margin of safety varies among samples. The lowest margin is observed in sample 3 (Strength: 1,785 MPa, Stress: 1,185 MPa), while the highest margin occurs in sample 14 (Strength: 1930 MPa, Stress: 1330 MPa). This dataset provides a foundation for conducting a stress-strength reliability analysis, where the probability that a structure's strength exceeds its applied stress ($R(X_2 < X_1)$) can be determined. Such analysis is crucial in aerospace engineering to assess the likelihood of failure and optimize material selection to ensure structural integrity under operational conditions.

In aerospace engineering, selecting materials that can withstand high stress while maintaining structural integrity is crucial. One widely used material is Carbon Fiber-Reinforced Polymer (CFRP), known for its high strength-to-weight ratio. The reliability of CFRP under operational stress is essential in ensuring safety and durability. The stress-strength reliability model is used to evaluate whether a material can endure applied stress without failure. Given two random variables: X_1which refers to the breaking strength of CFRP and X_2 which refers to the operational stress applied to the material. A study was conducted on CFRP panels used in aircraft structures, where X_1 follows an EGFrP distribution with estimated parameters $(\alpha_1, \beta_1, \lambda_1)$. Also, the X_2 follows an EGFrP distribution with parameters $(\alpha_2, \beta_2, \lambda_2)$. Using real experimental data and the result in (20) CFRP specimens, the estimated reliability index was found to be

$$R(X_2 < X_1) \approx 0.92.$$

Table 11: Strength and Stress data in MPa
for 15 hypothetical aerospace structures samples.

Sample	X_1 (Strength (MPa))	X_2 (Stress (MPa))
1	1800	1200
2	1850	1250
3	1785	1185
4	1825	1225
5	1900	1300
6	1880	1280
7	1865	1265
8	1925	1325
9	1835	1235
10	1910	1310
11	1895	1295
12	1815	1215
13	1875	1275
14	1930	1330
15	1845	1245

A reliability index of 92% suggests CFRP is highly suitable for aerospace applications, minimizing the likelihood of catastrophic failure. The Hill estimator was applied to assess the tail behavior of the breaking strength distribution. Results showed a heavy-tailed nature, indicating rare but severe failures. Engineers must incorporate safety factors to mitigate extreme cases. Alternative materials, such as Titanium alloys, could be compared using $R(X_2 < X_1)$ to balance performance, weight, and cost in aircraft design.

12. Conclusions, limitations and future points

In this work, a new compound extension of the Fréchet distribution is introduced and studied. Some of its properties including moments, incomplete moments, quantile, random number generation, probability weighted moments, moment generating function, stress strength reliability model, residual life and reversed residual life functions are derived. 3-dimentional plots of skewness and kurtosis of the new model are presented for illustrating the flexibility of the new model. We presented a comprehensive simulation study designed to evaluate and compare the performance of certain five estimation methods under varying sample sizes. The primary objective is to assess the accuracy and consistency of these methods in estimating parameters of a given distribution, as measured by the mean squared error (MSE). The simulation is conducted for three different sample sizes: n =50, n =100, and n =200, allowing us to examine how the performance of each method evolves with increasing data availability. Two real applications are presented to compare estimation methods, using datasets on carbon fiber breaking stress and glass fiber strengths. Additionally, two more applications evaluate competitive statistical models, focusing on their ability to describe underlying distributions in reliability and extreme value analysis. Finally, the Hill estimator is applied to estimate the tail index of the new exponentiated generalized G Poisson model using the carbon fiber breaking stress data, providing insights into the dataset's heavy-tailed behavior. This comprehensive approach not only highlights the strengths and limitations of various methods and models but also offers practical guidance for selecting appropriate techniques in real applications. The study underscores the importance of robust statistical tools for accurate modeling and inference. Based on a reliability analysis of composite materials for aerospace applications (case study), with a 92% reliability index, CFRP exhibits strong performance in aerospace applications. However, engineers should consider additional safety margins to mitigate extreme stress scenarios, particularly given the heavy-tailed behavior of the breaking strength distribution. The Hill estimator analysis indicates a heavy-tailed nature in CFRP strength distribution, meaning that while failures are rare, they can be

catastrophic. While CFRP offers an excellent strength-to-weight ratio, alternative materials such as Titanium alloys or hybrid composites should be evaluated using the same stress-strength reliability approach.

The EGFrP model, while offering significant flexibility and improved fitting capabilities for heavy-tailed data, has several limitations that must be considered. One primary concern is its applicability to light-tailed data, where its structure may not provide the best fit compared to alternative models designed for such distributions. Additionally, parameter identifiability issues can arise due to the complexity of the model, leading to multiple parameter sets producing similar likelihood values, particularly in cases with limited data. The model is also sensitive to initial parameter values, meaning improper starting points in estimation procedures like MLE can result in convergence difficulties or suboptimal parameter estimates. Moreover, the added flexibility of the EGFrP model comes at the cost of higher computational complexity, requiring substantial processing power, especially for iterative estimation techniques such as bootstrapping or Bayesian approaches. Another potential concern is overfitting, as the presence of multiple parameters increases the risk of capturing noise rather than true underlying data patterns, particularly in small sample scenarios. To mitigate this, careful model selection criteria, such as AIC and BIC, should be used. Finally, this paper assumes data suitability for the EGFrP model, but in real applications, it is crucial to ensure that the dataset aligns well with the distribution's assumptions before selecting it as the optimal modeling choice.

Main Abbreviations

RV	Random Variable.
PMF	Probability mass function.
CDF	Cumulative distribution function.
iid RV	Independent and Identically Distributed Random Variables
Fr	Fréchet distribution
PDF	Probability Density Function
IE	Inverse Exponential Distribution
WFr	Weibull Fréchet
VaR	Value at Risk
IR	Inverse Rayleigh
EGGP	Exponentiated Generalized G Poisson Class
EGP	exponentiated G Poisson Class
Boot.	Bootstrapping estimation
EGFrP	exponentiated generalized Fréchet Poisson
KE	Kolmogorov estimates method
CVME	Cramér–von Mises estimation method
MSE	The mean squared error
MLE	maximum likelihood estimation method
KE	Kolmogorov Estimation Method
TIx	Tail Index
PWMs	Probability Weighted Moments
MGF	Moment Generating Function
CFRP	carbon fiber-reinforced polymer
AD2LE	Anderson–Darling left-tail of the second order estimation Method
AI_C	Akaike Information Criterion
HQI_C	Hannan-Quinn Information Criterion
CAI_C	Consistent Akaike Information Criterion)
BI_C	Bayesian information criterion
KDE	Kernel Density Estimation
TTT	Total Time on Test
P-P	Probability-Probability
QQ	quantile-quantile

Acknowledgment

This work was supported by the Deanship of Scientific Research, Vice Presidency for Graduate Studies and Scientific Research, King Faisal University, Saudi Arabia [Grant No. KFU251445].

REFERENCES

1. Aarset, M. V. (1987). How to identify a bathtub hazard rate. IEEE Transactions on Reliability, 36, 106-108.
2. Abiad, M., Alsadat, N., Abd El-Raouf, M. M., Yousof, H. M., & Kumar, A. (2025). Different copula types and reliability applications for a new fisk probability model. Alexandria Engineering Journal, 110, 512-526.
3. Abdelaziz, M. A., Nofal, Z. M., & Afify, A. Z. (2024). A Unified Family for Generating Probabilistic Models: Properties, Bayesian and Non-Bayesian Inference with Real-Data Applications. Pakistan Journal of Statistics and Operation Research, 20(4), 633-660. https://doi.org/10.18187/pjsor.v20i4.4741
4. Aboraya, M. (2021). Marshall-Olkin Lehmann Lomax distribution: theory, statistical properties, copulas and real data modeling. Pakistan Journal of Statistics and Operation Research, 509-530.
5. Aboraya, M., Ali, M. M., Yousof, H. M., & Mohamed, M. I. (2022). A new flexible probability model: Theory, estimation and modeling bimodal left skewed data. Pakistan Journal of Statistics and Operation Research, 437-463.
6. Afify, A. Z., Pescim, R. R., Cordeiro, G. M., & Mahran, H. A. (2023). A New Heavy-Tailed Exponential Distribution: Inference, Regression Model and Applications. Pakistan Journal of Statistics and Operation Research, 19(3), 395-411. https://doi.org/10.18187/pjsor.v19i3.4230
7. Aidi, K., Butt, N. S., Ali, M. M., Ibrahim, M., Yousof, H. M. and Shehata, W. A. M. (2021). A Modified Chi-square Type Test Statistic for the Double Burr X Model with Applications to Right Censored Medical and Reliability Data. Pakistan Journal of Statistics and Operation Research, 17(3), 615-623.
8. Aldahlan, M. A., Rabie, A. M., Abdelhamid, M., Ahmed, A. H. N., & Afify, A. Z. (2023). The Marshall–Olkin Pareto Type-I Distribution: Properties, Inference under Complete and Censored Samples with Application to Breast Cancer Data. Pakistan Journal of Statistics and Operation Research, 19(4), 603-622. https://doi.org/10.18187/pjsor.v19i4.4317
9. Algamal, Z. Y., & Basheer, G. (2021). Reliability Estimation of Three Parameters Weibull Distribution based on Particle Swarm Optimization. Pakistan Journal of Statistics and Operation Research, 17(1), 35-42. https://doi.org/10.18187/pjsor.v17i1.2354
10. Aljadani, A., Mansour, M. M., & Yousof, H. M. (2024). A Novel Model for Finance and Reliability Applications: Theory, Practices and Financial Peaks Over a Random Threshold Value-at-Risk Analysis. Pakistan Journal of Statistics and Operation Research, 20(3), 489-515. https://doi.org/10.18187/pjsor.v20i3.4439
11. Aljuhani, W., Klakattawi, H. S., & Baharith, L. A. (2022). Alpha Power Exponentiated New Weibull-Pareto Distribution: Its Properties and Applications. Pakistan Journal of Statistics and Operation Research, 18(3), 703-720. https://doi.org/10.18187/pjsor.v18i3.3937
12. Alkhayyat, S. L., Mohamed, H. S., Butt, N. S., Yousof, H. M., & Ali, E. I. (2023). Modeling the Asymmetric Reinsurance Revenues Data using the Partially Autoregressive Time Series Model: Statistical Forecasting and Residuals Analysis. Pakistan Journal of Statistics and Operation Research, 425-446.
13. Ali, M. M., Ali, I., Yousof, H. M. and Ibrahim, M. (2022). G Families of Probability Distributions: Theory and Practices. CRC Press, Taylor & Francis Group.
14. Ali, M. M., Imon, R., Ali, I. and Yousof, H. M. (2025). Statistical Outliers and Related Topics. CRC Press, Taylor & Francis Group.
15. Almazah, M.M.A., Almuqrin, M.A., Eliwa, M.S., El-Morshedy, M., Yousof, H.M. (2023). Modeling Extreme Values Utilizing an Asymmetric Probability Function. Symmetry 2021, 13, 1730. https://doi.org/10.3390/sym13091730
16. Almetwally, E. M., Afify, A. Z., & Hamedani, G. G. (2021). Marshall-Olkin Alpha Power Rayleigh Distribution: Properties, Characterizations, Estimation and Engineering applications. Pakistan Journal of Statistics and Operation Research, 17(3), 745-760. https://doi.org/10.18187/pjsor.v17i3.3473
17. Almongy , H. M., Almetwally, E. M., & Mubarak, A. E. (2021). Marshall-Olkin Alpha Power Lomax Distribution: Estimation Methods, Applications on Physics and Economics. Pakistan Journal of Statistics and Operation Research, 17(1), 137-153. https://doi.org/10.18187/pjsor.v17i1.3402
18. Alsultan, R. (2023). The Marshall-Olkin Pranav distribution: Theory and applications. Pakistan Journal of Statistics and Operation Research, 19(1), 155-166. https://doi.org/10.18187/pjsor.v19i1.4058
19. Aboraya, M. (2021). Marshall-Olkin Lehmann Lomax distribution: theory, statistical properties, copulas and real data modeling. Pakistan Journal of Statistics and Operation Research, 509-530.
20. Aboraya, M., Ali, M. M., Yousof, H. M. and Ibrahim, M. (2022). A New Flexible Probability Model: Theory, Estimation and Modeling Bimodal Left Skewed Data. Pakistan Journal of Statistics and Operation Research, 18(2), 437-463. https://doi.org/10.18187/pjsor.v18i2.3938
21. Ahmed, B., Chesneau, C. Ali, M. M. and Yousof, H. M. (2022). Amputated Life Testing for Weibull Reciprocal Weibull Percentiles: Single, Double and Multiple Group Sampling Inspection Plans with Applications, Pakistan Journal of Statistics and Operation Research, 18(4), 995-1013.
22. Afify, A. Z., Yousof, H. M., Cordeiro, G. M., Ortega, E. M. M. and Nofal, Z. M. (2016). The Weibull Fréchet distribution and its applications. Journal of Applied Statistics, 43, 2608–2626.
23. Ahmed, B., & Yousof, H. M. (2023). A new group acceptance sampling plans based on percentiles for the Weibull Fréchet model. Statistics, Optimization & Information Computing, 11(2), 409-421.
24. Al-Babtain, A. A. Elbatal, I. and Yousof, H. M. (2020). A new three parameter Fréchet model with mathematical properties and applications. Journal of Taibah University for Science, 14, 265–278.

25. Aryal, G. R. and Yousof, H. M. (2017). The exponentiated generalized-G Poisson family of distributions. Stochastics and Quality Control, 32, 1-17.
26. Alizadeh, M., Afshari, M., Contreras-Reyes, J. E., Mazarei, D., & Yousof, H. M. (2024). The Extended Gompertz Model: Applications, Mean of Order P Assessment and Statistical Threshold Risk Analysis Based on Extreme Stresses Data. IEEE Transactions on Reliability, doi: 10.1109/TR.2024.3425278.
27. Alizadeh, M., Afshari, M., Cordeiro, G. M., Ramaki, Z., Contreras-Reyes, J. E., Dirnik, F., & Yousof, H. M. (2025). A New Weighted Lindley Model with Applications to Extreme Historical Insurance Claims. Stats, 8(1), 8.
28. Altun, E. Alizadeh, M., Yousof, H. M., Rasekhi, M. and Hamedani, G. G. (2021). A New Type II Half Logistic-G family of Distributions with Properties, Regression Models, Reliability Systems and Applications. Applications and Applied Mathematics: An International Journal, 16(2), 823-843.
29. Benkhelifa, L. (2022). The Beta Power Muth Distribution: Regression Modeling, Properties and Data Analysis. Pakistan Journal of Statistics and Operation Research, 18(1), 225-243. https://doi.org/10.18187/pjsor.v18i1.3529
30. Bagci, K., Erdogan, N., Arslan, T., & Celik, H. E. (2022). Alpha power inverted Kumaraswamy distribution: Definition, different estimation methods, and application. Pakistan Journal of Statistics and Operation Research, 18(1), 13-25. https://doi.org/10.18187/pjsor.v18i1.3327
31. Bandar, S. A., Hussein, E. A., Yousof, H. M., Afify, A. Z., & Abdellatif, A. D. (2023). A NOVEL EXTENSION OF THE REDUCED-KIES FAMILY: PROPERTIES, INFERENCE, AND APPLICATIONS TO RELIABILITY ENGINEERING DATA. Advanced Mathematical Models & Applications, 8(1).
32. Barreto-Souza, W.M.; Cordeiro, G.M.; Simas, A.B. (2011). Some results for beta Fréchet distribution. Commun. Stat. Theory Methods, 40, 798–811.
33. Chettri, S., Das, B., Imliyangba, I., & Hazarika, P. J. (2022). A Generalized Form of Power Transformation on Exponential Family of Distribution with Properties and Application. Pakistan Journal of Statistics and Operation Research, 18(3), 511-535. https://doi.org/10.18187/pjsor.v18i3.3883
34. Daghistani, A. M., Al-Zahrani, B., & Shahbaz, M. Q. (2023). A New Inverse Kumaraswamy Family of Distributions: Properties and Application. Pakistan Journal of Statistics and Operation Research, 19(2), 313-326. https://doi.org/10.18187/pjsor.v19i2.4295
35. Elgohari, H. and Yousof, H. M. (2021). A New Extreme Value Model with Different Copula, Statistical Properties and Applications. Pakistan Journal of Statistics and Operation Research, 17(4), 1015-1035. https://doi.org/10.18187/pjsor.v17i4.3471
36. Elbatal, I., & Aldukeel, A. (2021). On Erlang-Truncated Exponential Distribution: Theory and Application. Pakistan Journal of Statistics and Operation Research, 17(1), 155-168. https://doi.org/10.18187/pjsor.v17i1.2963
37. Elsayed, H. A. H. and Yousof, H. M. (2020). The generalized odd generalized exponential Fréchet model: Univariate, bivariate and multivariate extensions with properties and applications to the univariate version. Pak. J. Stat. Oper. Res., 16, 529–544.
38. ElSherpieny, E. A., & Almetwally, E. M. (2022). The Exponentiated Generalized Alpha Power Family of Distribution: Properties and Applications. Pakistan Journal of Statistics and Operation Research, 18(2), 349-367. https://doi.org/10.18187/pjsor.v18i2.3515
39. Fisher, R. A. and Tippett, L. H. C. (1928). Limiting forms of the frequency distribution of the largest or smallest member of a sample. In Mathematical Proceedings of the Cambridge Philosophical Society, pages 180–190. Cambridge Univ Press.
40. Gabanakgosi, M., & Oluyede, B. (2024). The Topp-Leone-Gompertz-G Power Series Class of Distributions with Applications: Topp-Leone-Gompertz-G Power Series Class of Distributions . Pakistan Journal of Statistics and Operation Research, 20(2), 171-195. https://doi.org/10.18187/pjsor.v20i2.4032
41. Fréchet, M. (1927). Sur la loi de probabilit´e de l´ecart maximum. Ann. de la Soc. polonaisede Math, 6, 93–116.
42. Gnedenko, B. (1943). Sur la distribution limite du terme maximum d'une serie aleatoire. Annals of Mathematics, Volume 44.
43. Hamed, M. S., Cordeiro, G. M. and Yousof, H. M. (2022). A New Compound Lomax Model: Properties, Copulas, Modeling and Risk Analysis Utilizing the Negatively Skewed Insurance Claims Data. Pakistan Journal of Statistics and Operation Research, 18(3), 601-631. https://doi.org/10.18187/pjsor.v18i3.3652
44. Hamedani, G. G., Korkmaz, M. C., Butt, N. S. and Yousof, H. M. (2021). The Type I Quasi Lambert Family: Properties, Characterizations and Different Estimation Methods. Pakistan Journal of Statistics and Operation Research, 17(3), 545-558.
45. Hamedani, G., Korkmaz, M. C., Butt, N. S., & Yousof, H. M. (2022). The Type II Quasi Lambert G Family of Probability Distributions. Pakistan Journal of Statistics and Operation Research, 18(4), 963-983. https://doi.org/10.18187/pjsor.v18i4.3907
46. Haq, M. A. ul, Yousof, H. M., & Hashmi, S. (2017). A New Five-Parameter Fréchet Model for Extreme Values. Pakistan Journal of Statistics and Operation Research, 13(3), 617-632.
47. Hashem, A. F., Alotaibi, N., Alyami, S. A., Abdelkawy, M. A., Elgawad, M. A. A., Yousof, H. M., & Abdel-Hamid, A. H. (2024). Utilizing Bayesian inference in accelerated testing models under constant stress via ordered ranked set sampling and hybrid censoring with practical validation. Scientific Reports, 14(1), 14406.
48. Hassan, A., Dar, I. H., & Lone, M. A. (2024). A new class of probability distributions with an application in engineering science. Pakistan Journal of Statistics and Operation Research, 20(2), 217-231. https://doi.org/10.18187/pjsor.v20i2.3845
49. Ibrahim, M., Aidi, K., Ali, M. M. and Yousof, H. M. (2023). A Novel Test Statistic for Right Censored Validity under a new Chen extension with Applications in Reliability and Medicine. Annals of Data Science, 10(5):1285–1299.
50. Ibrahim, M., Ali, M. M., Goual, H., & Yousof, H. (2022). The Double Burr Type XII Model: Censored and Uncensored Validation Using a New Nikulin-Rao-Robson Goodness-of-Fit Test with Bayesian and Non-Bayesian Estimation Methods. Pakistan Journal of Statistics and Operation Research, 18(4), 901-927. https://doi.org/10.18187/pjsor.v18i4.3600
51. Ibrahim, M., Hamedani, G. G., Butt, N. S. and Yousof, H. M. (2022). Expanding the Nadarajah Haghighi Model: Copula, Censored and Uncensored Validation, Characterizations and Applications. Pakistan Journal of Statistics and Operation Research, 18(3), 537-553. https://doi.org/10.18187/pjsor.v18i3.3420
52. Ibrahim, M., Ansari, S. I., Al-Nefaie, A. H., & Yousof, H. M. (2025). A New Version of the Inverse Weibull Model with Properties, Applications and Different Methods of Estimation. Statistics, Optimization & Information Computing, 13(3), 1120-1143. https://doi.org/10.19139/soic-2310-5070-1658
53. Ibrahim, M., Butt, N. S., Al-Nefaie, A. H., Hamedani, G. G., Yousof, H. M., & Mahmoud, A. S. (2025). An Extended Discrete Model for Actuarial Data and Value at Risk Analysis: Properties, Applications and Risk Analysis under Financial Automobile Claims Data.

Statistics, Optimization & Information Computing, 13(1), 27-46.
54. Ibrahim. M., Handique, L., Chakraborty, S., Butt, N. S. and M. Yousof, H. (2021). A new three-parameter xgamma Fréchet distribution with different methods of estimation and applications. Pakistan Journal of Statistics and Operation Research, 17(1), 291-308. https://doi.org/10.18187/pjsor.v17i1.2887
55. Jahanshahi, S.M.A., Yousof, H. M. and Sharma, V.K. (2019). The Burr X Fréchet Model for Extreme Values: Mathematical Properties, Classical Inference and Bayesian Analysis. Pak. J. Stat. Oper. Res., 15(3), 797-818.
56. Khalil, M. G., & Ali, E. I. A. (2023). A Generalization of Burr Type XII Distribution with Properties, Copula and Modeling Symmetric and Skewed Real Data Sets: A Generalization of Burr Type XII Distribution. Pakistan Journal of Statistics and Operation Research, 19(1), 77-101. https://doi.org/10.18187/pjsor.v19i1.3377
57. Korkmaz, M. C., Alizadeh, M., Yousof, H. M. and Butt, N. S. (2018). The generalized odd Weibull generated family of distributions: statistical properties and applications. Pak. J. Stat. Oper. Res., 14, 541-556.
58. Korkmaz, M. C., Altun, E., Yousof, H. M. and Hamedani G. G. (2019). The Odd Power Lindley Generator of Probability Distributions: Properties, Characterizations and Regression Modeling, International Journal of Statistics and Probability, 8. 70-89.
59. Korkmaz, M. C. Yousof, H. M. and Ali, M. M. (2017). Some Theoretical and Computational Aspects of the Odd Lindley Fréchet Distribution, Journal of Statisticians: Statistics and Actuarial Sciences, 2, 129-140.
60. Nadarajah, S. and Kotz, S. (2003). The exponentiated Fréchet distribution, Interstat Electron. Journal, (2003), 1–7.
61. Kotz, S. and Johnson, N. L. (1992). Breakthroughs in Statistics: Foundations and basic theory. Springer,Volume 1.
62. Malik, A. S., & Ahmad, S. (2022). A New Transmuted Weibull Distribution: Properties and Application. Pakistan Journal of Statistics and Operation Research, 18(2), 369-381. https://doi.org/10.18187/pjsor.v18i2.2728
63. Mansour, M. M., Ibrahim, M., Aidi, K., Butt, N. S., Ali, M. M., Yousof, H. M., & Hamed, M. S. (2020). A New Log-Logistic Lifetime Model with Mathematical Properties, Copula, Modified Goodness-of-Fit Test for Validation and Real Data Modeling. Mathematics, 8(9), 1508.
64. Mansour, M. M., Butt, N. S., Ansari, S. I., Yousof, H. M., Ali, M. M., & Ibrahim, M. (2020). A new exponentiated Weibull distribution's extension: copula, mathematical properties and applications. Contributions to Mathematics, 1 (2020) 57–66. DOI: 10.47443/cm.2020.0018
65. Mansour, M., Korkmaz, M. Ç., Ali, M. M., Yousof, H. M., Ansari, S. I., & Ibrahim, M. (2020). A generalization of the exponentiated Weibull model with properties, Copula and application. Eurasian Bulletin of Mathematics, 3(2), 84-102.
66. Mansour, M., Rasekhi, M., Ibrahim, M., Aidi, K., Yousof, H. M., & Elrazik, E. A. (2020). A New Parametric Life Distribution with Modified Bagdonavičius–Nikulin Goodness-of-Fit Test for Censored Validation, Properties, Applications, and Different Estimation Methods. Entropy, 22(5), 592.
67. Mansour, M., Yousof, H. M., Shehata, W. A. M., & Ibrahim, M. (2020). A new two parameter Burr XII distribution: properties, copula, different estimation methods and modeling acute bone cancer data. Journal of Nonlinear Science and Applications, 13(5), 223-238.
68. Mansour, M. M., Butt, N. S., Yousof, H. M., Ansari, S. I., & Ibrahim, M. (2020). A Generalization of Reciprocal Exponential Model: Clayton Copula, Statistical Properties and Modeling Skewed and Symmetric Real Data Sets. Pakistan Journal of Statistics and Operation Research, 16(2), 373-386.
69. Minkah, R., de Wet, T., Ghosh, A., & Yousof, H. M. (2023). Robust extreme quantile estimation for Pareto-type tails through an exponential regression model. Communications for Statistical Applications and Methods, 30(6), 531-550.
70. Nichols, M. D, Padgett, W. J. (2006). A Bootstrap control chart for Weibull percentiles. Quality and Reliability Engineering International, 22, 141-151.
71. Oluyede, B., Peter, P. O., Ndwapi, N., & Bindele, H. (2022). The Exponentiated Half-logistic Odd Burr III-G: Model, Properties and Applications: The Exponentiated Half-logistic Odd Burr III-G. Pakistan Journal of Statistics and Operation Research, 18(1), 33-57. https://doi.org/10.18187/pjsor.v18i1.3668
72. Rana, M. S., Shahbaz, S. H., Shahbaz, M. Q., & Rahman, M. M. (2022). Pareto-weibull distribution with properties and applications: a member of pareto-X family. Pakistan Journal of Statistics and Operation Research, 121-132.
73. Refaie, M. K., & Ali, E. I. (2023). A New Reciprocal System of Burr Type X Densities with Applications in Engineering, Reliability, Economy, and Medicine. Pakistan Journal of Statistics and Operation Research, 373-394.
74. Refaie, M. K., Butt, N. S., & Ali, E. I. (2023). A new probability distribution: properties, copulas and applications in medicine and engineering. Pakistan Journal of Statistics & Operation Research, 19(2).
75. Refaie, M. K., Yaqoob, A. A., Selim, M. A., & Ali, E. I. (2023). A Novel Version of the Exponentiated Weibull Distribution: Copulas, Mathematical Properties and Statistical Modeling. Pakistan Journal of Statistics and Operation Research, 491-519.
76. Rasekhi, M., Saber, M. M., & Yousof, H. M. (2020). Bayesian and classical inference of reliability in multicomponent stress-strength under the generalized logistic model. Communications in Statistics-Theory and Methods, 50(21), 5114-5125.
77. Rasekhi, M., Saber, M., Yousof, H. M., & Ali, E. I. (2024). Estimation of the Multicomponent Stress-Strength Reliability Model Under the Topp-Leone Distribution: Applications, Bayesian and Non-Bayesian Assessment. Statistics, Optimization & Information Computing, 12(1), 133-152.
78. Saber, M. M. Marwa M. Mohie El-Din and Yousof, H. M. (2022). Reliability estimation for the remained stress-strength model under the generalized exponential lifetime distribution, Journal of Probability and Statistics, 2021, 1-10.
79. Saber, M. M., Rasekhi, M. and Yousof, H. M. (2022). Generalized Stress-Strength and Generalized Multicomponent Stress-Strength Models. Statistics, Optimization & Information Computing, forthcoming.
80. Salah, M. M., El-Morshedy, M.; Eliwa, M. S. and Yousof, H. M. (2020). Expanded Fréchet model: mathematical properties, copula, different estimation methods, applications and validation testing. mathematics, 8, 1949.
81. Salem, M., Emam, W., Tashkandy, Y., Ibrahim, M., Ali, M. M., Goual, H., & Yousof, H. M. (2023). A new Lomax extension: Properties, risk analysis, censored and complete goodness-of-fit validation testing under left-skewed insurance, reliability and medical data. Symmetry, 15(7), 1356.
82. Silva, R. V. D., de Andrade, T. A., Maciel, D., Campos, R. P., and Cordeiro, G. M. (2013). A new lifetime model: The gamma extended Fréchet distribution. Journal of Statistical Theory and Applications, 12, 39-54.

83. Shehata, W. A. M., Aljadani, A., Mansour, M. M., Alrweili, H., Hamed, M. S., & Yousof, H. M. (2024). A Novel Reciprocal-Weibull Model for Extreme Reliability Data: Statistical Properties, Reliability Applications, Reliability PORT-VaR and Mean of Order P Risk Analysis. Pakistan Journal of Statistics and Operation Research, 20(4), 693-718. https://doi.org/10.18187/pjsor.v20i4.4302
84. Shehata, W. A. M. and Yousof, H. M. (2021). The four-parameter exponentiated Weibull model with Copula, properties and real data modeling. Pakistan Journal of Statistics and Operation Research, 17(3), 649-667.
85. Shehata, W. A. M., Butt, N. S., Yousof, H., & Aboraya, M. (2022). A New Lifetime Parametric Model for the Survival and Relief Times with Copulas and Properties. Pakistan Journal of Statistics and Operation Research, 18(1), 249-272.
86. Shehata, W. A., Goual, H., Hamida, T., Hiba, A., Hamedani, G. G., Al-Nefaie, A. H., Ibrahim, M., Butt, N. S., Osman, R. M. A., and Yousof, H. M. (2024). Censored and Uncensored Nikulin-Rao-Robson Distributional Validation: Characterizations, Classical and Bayesian estimation with Censored and Uncensored Applications. Pakistan Journal of Statistics and Operation Research, 20(1), 11-35.
87. Shehata, W. A. M., Yousof, H. M., & Aboraya, M. (2021). A Novel Generator of Continuous Probability Distributions for the Asymmetric Left-skewed Bimodal Real-life Data with Properties and Copulas. Pakistan Journal of Statistics and Operation Research, 17(4), 943-961. https://doi.org/10.18187/pjsor.v17i4.3903
88. Smith, R. L. and Naylor, J. C. (1987). A comparison of maximum likelihood and Bayesian estimators for the three-parameter Weibull distribution. Applied Statistics, 36, 358-369.
89. Teghri, S., Goual, H., Loubna, H., Butt, N. S., Khedr, A. M., Yousof, H. M., Ibrahim, M. & Salem, M. (2024). A New Two-Parameters Lindley-Frailty Model: Censored and Uncensored Schemes under Different Baseline Models: Applications, Assessments, Censored and Uncensored Validation Testing. Pakistan Journal of Statistics and Operation Research, 109-138.
90. ul Haq, M. A., Afify, A. Z., Al-Mofleh, H., Usman, R. M., Alqawba, M., & Sarg, A. M. (2021). The Extended Marshall-Olkin Burr III Distribution: Properties and Applications. Pakistan Journal of Statistics and Operation Research, 1-14.
91. Yousof, H.M.; Tashkandy, Y.; Emam, W.; Ali, M.M.; Ibrahim, M. A New Reciprocal Weibull Extension for Modeling Extreme Values with Risk Analysis under Insurance Data. Mathematics 2023, 11, 966. https://doi.org/10.3390/ math11040966
92. Verster, A., & Mbongo, S. (2024). Topp-Leone generalization of the Generalized Pareto distribution and its impact on Extreme value modelling. Pakistan Journal of Statistics and Operation Research, 20(4), 771-784. https://doi.org/10.18187/pjsor.v20i4.4593
93. Von-Mises, R. (1936). La distribution de la plus grande de n valeurs. Rev. math. Union interbalcanique, 1, 141-160.
94. Von-Mises, R. (1964). Selected papers of Richard von Mises, American mathematical society, 2, 271-294.
95. Yousof, H. M., Afify, A. Z., Alizadeh, M., Butt, N. S., Hamedani, G. G. and Ali, M. M. (2015). The transmuted exponentiated generalized-G family of distributions. Pak. J. Stat. Oper. Res., 11, 441-464.
96. Yousof, H. M., Afify, A. Z., Ebraheim, A. N., Hamedani, G. G. and Butt, N. S. (2016). On six-parameter Fréchet distribution: properties and applications, Pak. J. Stat. Oper. Res., 12, 281-299.
97. Yousof, H. M., Ali, M. M., Aidi, K., Ibrahim, M. (2023). The modified Bagdonavičius-Nikulin goodness-of-fit test statistic for the right censored distributional validation with applications in medicine and reliability. Statistics in Transition New Series, 24(4), 1-18.
98. Yousof, H. M., Aidi, K., Hamedani, G. G and Ibrahim, M. (2021). A new parametric lifetime distribution with modified Chi-square type test for right censored validation, characterizations and different estimation methods. Pakistan Journal of Statistics and Operation Research, 17(2), 399-425.
99. Yousof, H. M., Altun, E. and Hamedani, G. G. (2018a). A new extension of Frechet distribution with regression models, residual analysis and characterizations. Journal of Data Science, 16, 743-770.
100. Yousof, H. M., Aljadani, A., Mansour, M. M., & Abd Elrazik, E. M. (2024). A New Pareto Model: Risk Application, Reliability MOOP and PORT Value-at-Risk Analysis. Pakistan Journal of Statistics and Operation Research, 20(3), 383-407. https://doi.org/10.18187/pjsor.v20i3.4151
101. Yousof, H. M., Al-nefaie, A. H., Aidi, K., Ali, M. M., & Ibrahim, M. (2021). A Modified Chi-square Type Test for Distributional Validity with Applications to Right Censored Reliability and Medical Data. Pakistan Journal of Statistics and Operation Research, 17(4), 1113-1121. https://doi.org/10.18187/pjsor.v17i4.3899
102. Yousof, H. M., Al-Nefaie, A. H., Butt, N. S., Hamedani, G., Alrweili, H., Aljadani, A., Mansour, M. M., Hamed, M. S., & Ibrahim, M. (2024). A New Discrete Generator with Mathematical Characterization, Properties, Count Statistical Modeling and Inference with Applications to Reliability, Medicine, Agriculture, and Biology Data. Pakistan Journal of Statistics and Operation Research, 20(4), 745-770. https://doi.org/10.18187/pjsor.v20i4.4616
103. Yousof, H. M.; Butt, N. S.; Alotaibi, R. M.; Rezk, H.; Alomani, G. A.; Ibrahim, M. (2019). A new compound Fréchet distribution for modeling breaking stress and strengths data. Pak. J. Stat. Oper. Res., 1017–1035.
104. Yousof, H. M., Jahanshahi, S. M., Ramires, T. G Aryal, G. R. and Hamedani G. G. (2018b). A new distribution for extreme values: regression model, characterizations and applications. Journal of Data Science, 16, 677-706.
105. Yousof, H. M., Goual, H., Emam, W., Tashkandy, Y., Alizadeh, M., Ali, M. M., & Ibrahim, M. (2023). An Alternative Model for Describing the Reliability Data: Applications, Assessment, and Goodness-of-Fit Validation Testing. Mathematics, 11(6), 1308.
106. Yousof, H. M., Goual, H., Khaoula, M. K., Hamedani, G. G., Al-Aefaie, A. H., Ibrahim, M., ... & Salem, M. (2023). A novel accelerated failure time model: Characterizations, validation testing, different estimation methods and applications in engineering and medicine. Pakistan Journal of Statistics and Operation Research, 19(4), 691-717.
107. Yousof, H. M., Hamedani, G. G., & Ibrahim, M. (2020). The Two-parameter Xgamma Fréchet Distribution: Characterizations, Copulas, Mathematical Properties and Different Classical Estimation Methods. Contributions to Mathematics, 2 (2020), 32-41.
108. Yousof, H. M., Majumder, M., Jahanshahi, S. M. A., Ali, M. M. and Hamedani G. G. (2018c). A new Weibull class of distributions: theory, characterizations and applications, Journal of Statistical Research of Iran, 15, 45–83.
109. Yousof, H. M., Saber, M. M., Al-Nefaie, A. H., Butt, N. S., Ibrahim, M., & Alkhayyat, S. L. (2024). A discrete claims-model for the inflated and over-dispersed automobile claims frequencies data: Applications and actuarial risk analysis. Pakistan Journal of Statistics and Operation Research, 20(2), 261-284.